POLITECNICO DI TORINO

Collegio di Ingegneria Meccanica, Aerospaziale, dell'Autoveicolo e della Produzione

**Corso di Laurea Magistrale
in Ingegneria Aerospaziale**

Thesis of Master's Degree

Aeromechanical Model of Electric Wind Turbine with Fixed Wing

Supervisors

prof. Paolo Maggiore
prof. Matteo Davide Lorenzo Dalla Vedova

Candidate

Miguel López Alonso

March 2019

Abstract

The following thesis will describe the trajectory of a kite linked to the ground, with the purpose of producing wind power. The report will follow a typical technical structure that includes: introduction, state of the art, kite definition and requirements, mathematical model, code manual, results and conclusions.

In the introduction chapter, the influence of renewable energies and in particular wind energy will be discussed, as well as, the technologies for its exploitation. Then, will be analysed the state of the art of the high-altitude wind power, because the kite of the thesis will work at high altitudes. When the setting in which the kite will produce wind power has been defined, the definition of the kite and the hypothesis on its movement will be commented in the chapter 3.

In the mathematical model chapter, the equations and figures to understand the movement will be explained, as well as, the simplifications made. In the results chapter, a nominal movement of the kite will be discussed, as well as, a study of the wind to optimize the wind energy created.

To summarize, the conclusions of this project and some previous wrong steps will be commented, as well as, some future study to do to the next phase of the project.

Riassunto

La seguente tesi descriverà la traiettoria di un aquilone legato al terreno, con lo scopo di produrre energia eolica. Il rapporto seguirà una tipica struttura tecnica che include: introduzione, stato dell'arte, definizione e requisiti dell'aquilone, modello matematico, manuale del codice, risultati e conclusioni.

Nella introduzione verranno discusse l'influenza delle energie rinnovabili e in particolare l'energia eolica, e le tecnologie per il suo sfruttamento. Quindi, verrà analizzato lo stato dell'arte della energia eolica ad alta quota, perché l'aquilone della tesi funzionerà ad alta quota. Quando l'impostazione in cui l'aquilone produrrà energia eolica è stata definita, la definizione dell'aquilone e l'ipotesi sul suo movimento saranno commentate nel capitolo 3.

Nel capitolo del modello matematico verranno spiegate le equazioni e le figure per comprendere il movimento, e le semplificazioni apportate. Nel capitolo dei risultati, verrà discusso un movimento nominale dell'aquilone, ed oltre uno studio del vento per ottimizzare l'energia eolica creata.

Per riassumere, verranno commentate le conclusioni di questo progetto e alcuni precedenti passi errati, oltre alcuni studi futuri da fare alla fase successiva del progetto.

Index

List of figures

List of tables

Chapter 1 - Introduction: Wind power

1.1. Renewable energies

In a historical situation characterized by a rising oil price and an increasing awareness of environmental problems, the development of alternative technologies and their use become a necessity rather than a challenge.

Among the most promising and innovative projects is that of KITENERGY, which aims to compete with the current wind industry. There are several main reasons for these improvements. The KITENERGY generator is a wind farm with a vertical axis of rotation. This configuration eliminates the static and dynamic problems that prevent the towers from increasing in height and therefore in the power of traditional wind turbines, which have a horizontal axis and are therefore subjected to strong tilting moments due to the wind pressure on the blades. Moreover, at the same cost of the plant, this project intercepts a much wider wind front, since at ground level heights not reachable by the wind towers.

Technically, renewable energies are those sources of energy that by their intrinsic characteristic are regenerated or are not "exhaustible" in the scale of "human" time or in any case are perceived by man or society; more specifically, it can be said that their generation speed is higher than the speed of use.

The gradual development of renewable technology, coupled with the progressive increase in oil prices, has greatly reduced the gap in economic convenience between the two. At the same time, the Life Cycle Analysis (LCA) method has been perfected to determine energy yield (EROI) and to compare technologies on an objective bases and not linked to the economic fluctuations of the moment or to the hidden or obvious support of governments.

The main criticisms related to current renewable technologies are mainly due to the low production availability throughout the year, that is a low availability value understood as hours of operation at rated power on an annual basis. The resources that are exploited have, by their very nature, a cyclical or weakly predictable course determining, in the case of their massive use, the impossibility of managing the balance in the distribution network between the energy required and that produced; there is therefore a maximum limit for energy penetration.

As can be seen from the graph below, which shows estimates made by the International Energy Agency, the role of renewable energy in the world will remain marginal. They do not even seem to affect the possible uses of biomasses and biofuels for transport purposes, and the growth of hydropower appears to be completely exhausted, causing saturation of exploitable basins.

The energy from nuclear sources, waiting for twists in the field of fusion, does not take off and is instead considered as constant. The increase in energy demand will therefore be almost entirely at the expense of fossil fuels, with constant growth in coal, oil and natural gas.
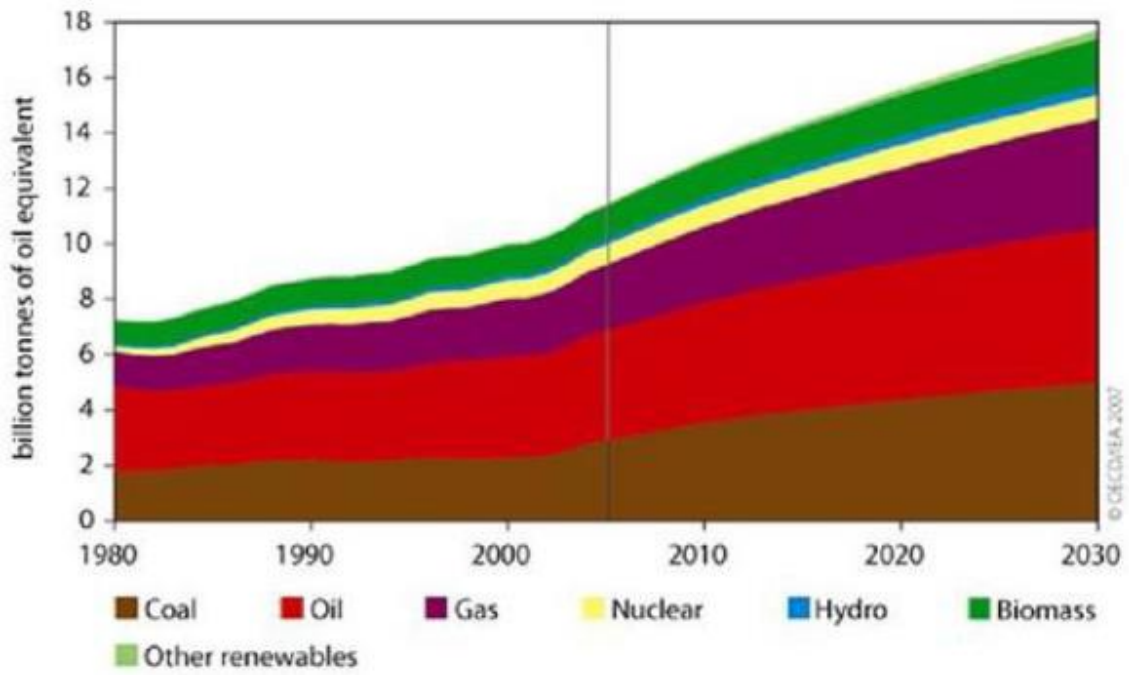
Figure 1.1: Comparative graph of renewable energy in the world overview.
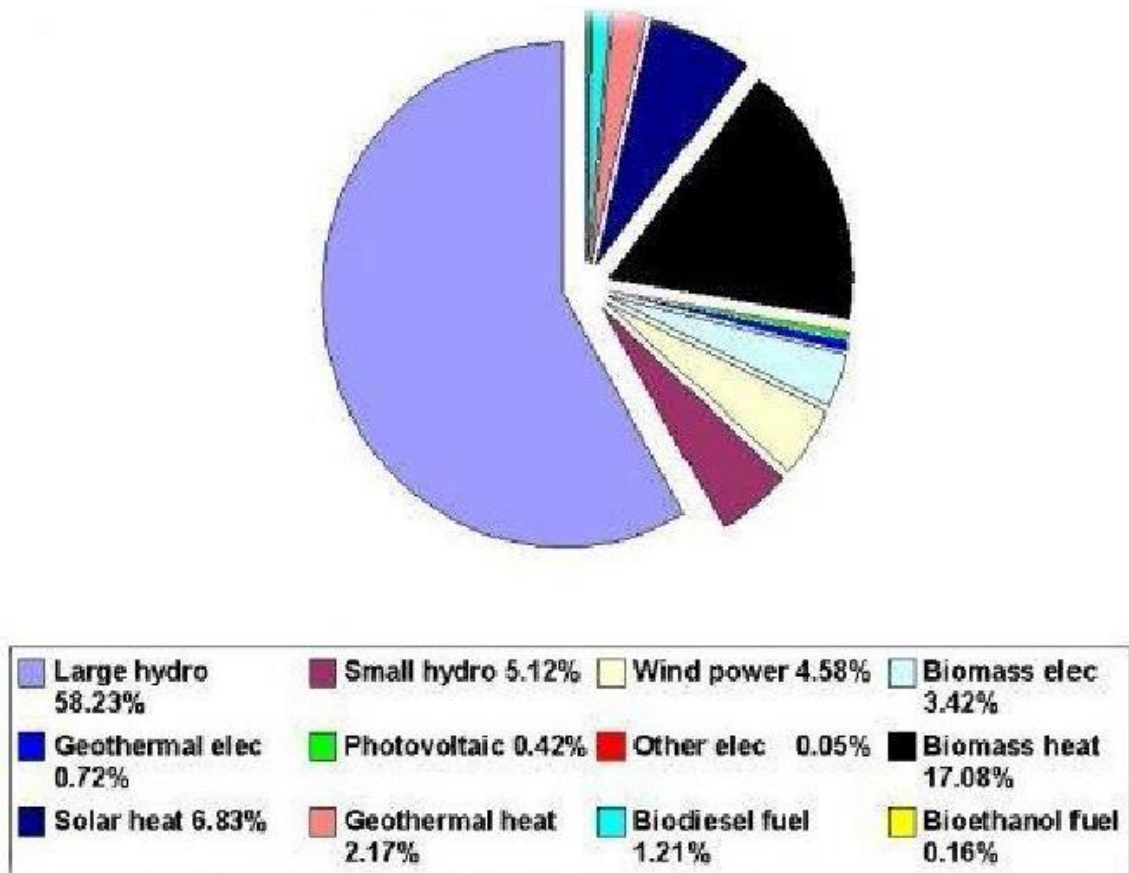
Figure 1.2: Pie chart on the relevance of various technologies worldwide.

The result of the zoom, in figure 1.2, on the portion of energy obtained from renewable sources carried out by Ren21 (Renewable Energy Policy Network for the 21st Century) shows what is the worldwide weight of each technology. If we exclude heat from wood and consider that hydroelectric power stations have exceeded the peak of installation in Italy as in other European countries, a predominant alternative technology cannot be registered.

1.2. The wind energy

Wind energy is the product of converting the kinetic energy of wind into other forms of energy. First, among all renewable sources for the cost-production ratio, it was also the first used by man. In the past, wind energy has been used immediately on site as a driving force for industrial and pre-industrial applications. It is currently being converted on a large scale into electricity through wind farms, consisting of a number of wind turbines located on towers. The "wind" resource; is in fact distributed in the atmosphere with increasing intensity as the altitude increases and concentrated mainly in two wind bands that completely envelop the Earth above the parallel that passes on Patagonia in the southern hemisphere and the other that passes on Europe. The average power of this belt, which ranges from about 500 metres to 10 000 metres above sea level and extends over 45 000 kilometres in width, is estimated at around 2 kW per m^2.

1.3. Technologies for the exploitation of wind energy

To date, there are various forms of technologies, more or less widespread, for the exploitation of wind energy. In general, some main categories of wind turbines can be distinguished:

- Wind turbine
- Micro-wind and small-wind systems
- Wind turbines for high altitude winds

1.3.1. The wind turbine

A wind turbine is a machine equipped with a rotor that, rotated by the wind, allows the production of electricity; the structure and operation of a turbine differs depending on the type of mechanism for energy production. In general, two types of turbines can be distinguished:

- Horizontal axis wind turbines: in which the rotor is oriented (actively or passively) parallel to the direction of origin of the wind.
- Vertical axis wind turbines: independent of the wind direction.

Figure 1.3: Wind turbine.

Wind turbines are used, in most cases, for the installation of so-called "wind farms", that are agglomerations of wind turbines within a circumscribed region. The economic expenditure and the environmental impact due to the necessary installation for the storage and transport of the energy produced, in fact, favor, to amortize the costs, the connection of several wind turbines. The wind farms can be of three types, depending on the area chosen for the installation:

Figure 1.4: On-shore wind farm.

• On-shore wind farm: This is the most widespread wind power, also for historical-technological reasons. The characteristics of on-shore wind power are typical of plants positioned on locations in general at least 3 km away from the nearest coast, typically on hills, heights or otherwise in open and windy areas. These plants cover a very wide range of power outputs (from 20 kW to 20 MW) and can be connected either to the "public" network or to an isolated network to power local users.

• Near-shore wind farm: it is a plant less than 3 km from the coast, typically inland, or on the sea but with distances that do not exceed 10 km from the coast. The sub-assembly that is installed on the mainland has characteristics similar to the on-shore in terms of production range (from 20 kW to 20 MW) while the set in the marine environment typically guarantees power produced in the order of MW.

Figure 1.5: Near-shore wind farm.

Figure 1.6: Off-shore wind farm.

• Off-shore wind farm: plant installed a few kilometres from the coast of seas or lakes, to better use the strong exposure to the currents of these areas. Some types of installation fall within the type of "floating wind turbine"; these turbines are mounted on a floating structure in order to work in areas very far from the coast characterized by deep seabed. The use of these turbines can be used, as well as for the production of electricity, also for the production of energy carriers, such as hydrogen and methanol, or for the distillation of sea water.

For the installation of wind farms, horizontal axis turbines are mainly used.

1.3.1.1. Vertical axis wind turbine

Figure 1.7: Horizontal axis wind turbine.

A wind generator with horizontal rotation axis on the ground (HAWT) is formed by a steel tower of heights between 60 and 100 meters on top of which there is an enclosure (nacelle) that contains an electric generator driven by a long-bladed rotor between 20 and 60 meters. It generates a very variable power, which can range from a few kW up to 5-6 MW, depending on the windiness of the place and time.

The horizontal axis generators require a minimum speed of $3 - 5 \, m \, / \, s$ (cut-in speed) and deliver the design power at a wind speed of $12 - 14 \, m \, / \, s$. At high speeds $(20/25 \, m \, / \, s)$ the aerogenerator is instead blocked by the braking system for safety reasons.

The traditional aerogenerators have, almost without exception, the horizontal axis of rotation. This feature is the main limit to the construction of machines much larger than those currently produced: the static and dynamic requirements that must be met do

Figure 1.8: Horizontal axis wind turbine components.

not allow to assume rotors with diameters much greater than 100 meters and tower heights greater than 180 meters. These dimensions concern machines for exclusive off-shore installation. The largest on-shore machines have rotor diameters of 70 meters and tower heights of 130 meters. In such a built machine the radius of the base exceeds 20 meters. The wind speed increases with the distance from the ground; this is the main reason why manufacturers of traditional wind turbines push the towers to such high altitudes. The growth of height, together with the diameter of the rotor that it makes possible, are the cause of the static complications of the whole machine, which imposes complex and expensive foundations and sophisticated strategies of protection in case of sudden gusts of wind too strong.

The main components of a wind turbine are the rotor, the gondola (or nacelle), and the tower. The horizontal axis rotors can be of three types:

- Single-blade rotor with counterweight: these are the most economical, but being unbalanced, they generate considerable mechanical stress and noise, and for this reason they are not widespread.
- Two-blade rotor: they have two blades placed at 180 ° to each other, then in the same direction but towards the opposite side. They have characteristics of cost and intermediate performance compared to the other two types and are the most common for smaller installations.
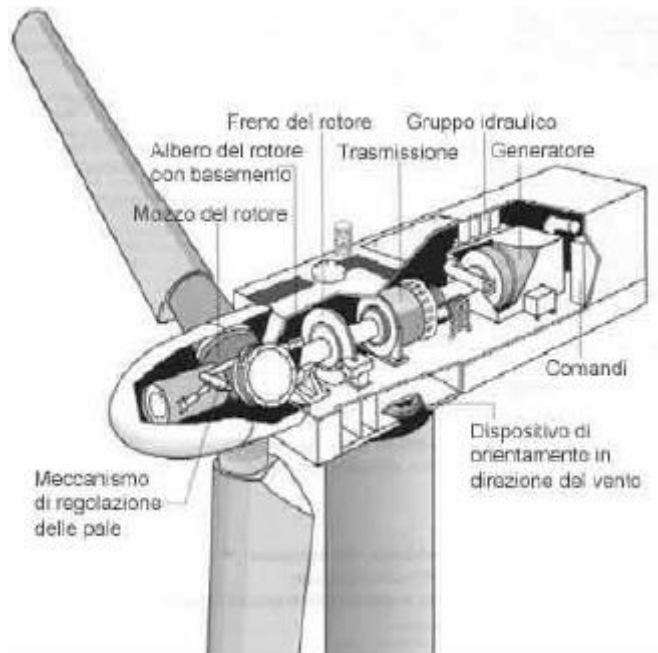
- Three-blade rotor: they have three blades placed at 120 ° one from the other. Despite being the most expensive, being balanced, they do not cause decomposed stress and are reliable and silent. The rotor shaft that transmits the motion is called the "slow shaft" or the main one. The most used blades are made of fibreglass or aluminium alloy. In the gondola (or nacelle) there is an electric generator, which is driven by the rotor; it is positioned on the top of the tower and can turn 180 ° on its axis, orientating itself in the appropriate direction according to that of the wind.

Figure 1.9: Horizontal axis wind turbine components.

In the cabin are located the various components of a wind turbine:

- the speed multiplier, because the electric generator produces electricity at the frequency of the electric network.
- the electric generator, which may be of the direct current or alternating current type.
- the control system, which is a generator interface device with the network and / or with any storage systems.

Small-sized wind turbines, under normal conditions, are self-directed by a simple rudder. Only in the most sophisticated are variable pitch blades installed, in order to adjust their inclination according to the wind speed to improve the yield. In small machines, the control system is usually passive, without servomotors acting on the angle of the paddles and on the angle between the nacelle and the wind:

- Stall control: the blades are built with torsion, so that at high wind speeds a stall starts on the blades, starting from the tip, spreading towards the centre. The active area of the blades decreases, thus decreasing the power.
- Passive yaw control: the system is dimensioned to automatically abandon the frontal attitude, in addition to a certain thrust of the wind.

The last element of the wind turbine is the tower for the suspension of the rotor and the nacelle. The tower can reach considerable dimensions in height up to 180 meters; typically as higher is the tower, the wind conditions are better in terms of intensity and constancy; as larger can be the rotor with an energy increase produced, the section can be wider; as more stable and well-designed must be the foundation in the ground, the costs are higher the and the impact on the landscape is worse. The materials used are frequently of a metallic type that guarantee maximum strength to mechanical internal stress due to external stresses during the operation of the aerogenerator.

1.3.1.2. Vertical axis wind turbine

A wind generator with vertical rotation axis on the ground (VAWT) is a type of wind machine characterized by a reduced quantity of moving parts in its structure, which gives it high resistance to strong gusts of wind and the possibility of exploiting any wind direction without having to orientate continuously. It is a very versatile machine, suitable both for domestic use and for the centralized production of electricity in the megawatt range (only one turbine satisfies the average electricity requirement of about 1000 houses). The substantially lower efficiency compared to those with horizontal axis (30%) has effectively confined

Figure 1.10: Vertical axis wind turbine.

the use in laboratories.

Wind magnetic turbine means a machine for the exploitation of wind energy using permanent magnets (e. g. neodymium) or superconducting electromagnets of the Maglev type, for transmission and/or for the reduction of friction experienced by the rotor and the axis of the main pinion of the aeronautical rotor.

Generators of this type can therefore work at low speeds (cut-in), but also at high speeds (cut-off) because they decrease the friction and the intense production of heat caused by it. As a consequence, they have an operating range of operation, in terms of the necessary wind conditions, much higher than the classic wind and at the same time also a much greater mechanical-electric conversion efficiency.

They also have reduced maintenance, because they do not need oil and gear change, and they experience about a quarter of the failures of a mechanical gearbox wind turbine, because they do not suffer many torque faults. These characteristics make it extremely interesting and revolutionary within the wind energy landscape.

The largest turbine of this type is the Liberty Wind Turbine, capable of producing 2.5 MW, built in the United States.

1.3.2. Micro-wind and small-wind systems

These are small systems, suitable for domestic use or to supplement the electricity consumption of small economic activities typically in stand-alone mode, that is the form of individual generators, which are then connected to the electricity grid (with a contribution to so-called distributed generation) or to storage systems. Usually these systems consist of horizontal axis wind turbines with a rotor diameter of 3 to 20 metres and a hub height of 10 to 20 metres. Usually small wind turbines are systems with a rated power between 20 kW and 200 kW, while micro wind turbines are systems with rated power less than 20 kW. The environmental impact of micro-wind has elements in common with that of large plants as it interferes with the same natural elements, while determining different perceptual results. The main advantages of micro-turbines compared to large wind turbines are:

- the greatly reduced size that engages limited spaces.
- the lack of need for support infrastructures.
- the reduced visibility of the system with consequent minor impact on the landscape.

Figure 1.11: Small wind turbine.

Despite these advantages, the wind plants installed in Italy today are almost exclusively large, also because they guarantee a more advantageous relationship between investment and profitability.

This problem could easily be overcome thanks to incentive programs. It should be noted that the amount of the percentage contribution necessary to make the investment economically attractive would be lower than the average allocated for photovoltaic panels that have a decidedly higher cost with the same kW installed. The micro-wind can be used for private civil or tourist infrastructures (farms, camps, shelters) isolated in the mountains, by the sea or on islands, not connected to the network. In fact, in these cases the often-high costs of grid connection are avoided. Other applications are related to the supply of telecommunication systems (repeaters, mobile telephony antennas installed remotely from the electricity network); pumping and drainage systems; public lighting utilities (streets, viaducts, tunnels, lights, traffic lights).

With the machines currently developed in Italy and abroad, the wind condition necessary for the installation of a plant can be identified with an average annual speed of not less than $4\ m\ /\ s$, but preferably higher than $6\ m\ /\ s$. The location of the turbine will have to be evaluated by taking stock of the problems that underlie its installation. On the one hand the proximity to the user can be penalizing for the functionality of the machine (interference to the wind due to the proximity of the buildings) as well as for the impact linked to the inevitable noise. On the other hand, the distance from the user increases the costs of wiring and burial of power lines as well as increasing the dispersion of energy. It is necessary to find a right agreement between the two requirements, also taking into account the importance of positioning the machine in a safe place.

1.3.3. Wind turbines for high altitude winds

A high-altitude wind turbine is a wind turbine that is located in the air without a tower, which can thus benefit from the higher wind speed almost constant at high altitudes, avoiding the construction cost and the problem of the encumbrance of towers or the need for rotating contacts or yaw mechanisms. As part of this technology, the objective of this thesis is to establish a nominal movement for the KITENERGY project discussed in the following chapters.

Chapter 2 - State of the art: high-altitude wind power

2.1. Wind turbines: problems and limits

Despite the increase in the continuous interest in wind energy and the various projects aimed above all at the construction of off-shore plants, the technology of wind turbines continues to not exceed some limitations inherent to the functioning of the mechanism and some problems related to the environmental impact.

First of all, there is a physical limit in the production of energy by a turbine; the maximum efficiency of a wind power plant, in fact, can be calculated using the Betz Law, which shows that the maximum energy that any generator can produce is 59.3% of that possessed by the wind that passes through it. This efficiency is the maximum achievable, and an aerogenerator with an efficiency of between 40% and 50% is considered optimal.

There are also technological limits, due to the length of the rotor blades, the height of the tower and the start of the mechanism. In fact, every system is characterized by a cut-in speed, so if the wind blows at a lower speed, the system does not produce energy. The height limit of the towers, therefore, does not allow to position the rotor at altitudes where the intensity of the winds is greater.

For this reason, the trend nowadays is to build off-shore parks, capable of exploiting more intense winds; remains, although less relevant than in the case of on-shore parks, the problem of intermittent winds and, therefore, of the variability of energy production. In addition to these problems, the greatest difficulty and the greatest maintenance burden for off-shore turbines are considered compared to those of on-shore parks.

Despite the good economic and energy prospects of wind farm projects, which allow large economies of scale, reducing the cost of the kilowatt hour of electricity, there is a major problem, especially for the approval and acceptance of these projects by society, the environmental impact, both visually and ecologically.

The large size of the towers and rotors of the turbines determine a large deterioration effect on the landscape; in fact, given the physical dimensions and the noise pollution, these structures must be built in places far from the inhabited centres, in natural areas where agriculture and grazing are also incompatible. A green colour, in an attempt to camouflage the aerogenerators within the landscape, minimizes the aesthetic problem.

With respect to the environmental impact of traditional energy sources, the impact of wind energy is relatively minor in terms of pollution. Wind energy does not consume fuel and does not emit air pollutants, unlike fossil energy sources.

The energy consumed to produce and transport the materials used to build a wind plant is equal to the new energy produced by the plant in the first months.

Ø = Rotor Diameter

5,000 kW
Ø 124m

2,000 kW
Ø 80m
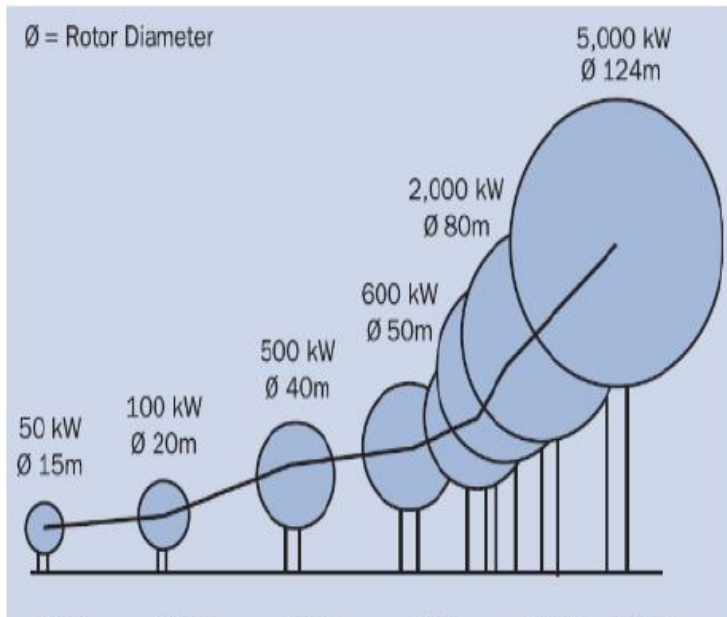
600 kW
Ø 50m

500 kW
Ø 40m

100 kW
Ø 20m

50 kW
Ø 15m

Figure 2.1: Total power generated over the years for a wind turbine.

From the figure on the side it can be seen how, in its twenty years of life, a wind turbine returns 70-75 times the energy needed to build it.

If wind turbines do not emit air pollutants, they produce noise pollution. By adopting a distance of a few hundred meters between a turbine and another, it is possible to reduce the noise and to obtain, near an aerogenerator, very low levels of noise, such as not to modify the background noise, which, at its time, it is strongly influenced by the wind itself.

The wind machine can also influence the propagation characteristics of telecommunications (like any obstacle), the quality of the connection in terms of signal-disturbance and the shape of the received signal with possible alteration of the information. The risk of such disturbances can be considered irrelevant for wind turbines that use blades made of non-metallic and anti-reflective material.

A last problem related to the presence of wind turbines is that which affects the fauna, in particular the volatile one. In addition to the collisions that can occur with birds of large size, there is an indirect deleterious effect: the wind farms in fact appear to be harmful to birds because they subtract the territory (the animals refuse to nest or feed in the wind farms) and for the barrier effect that forces the flocks to turn longer during the flights.

2.2.   Advantages on the exploitation of the wind in high altitude

Exploiting high altitude winds is a complicated but promising challenge. The first and greatest advantage of working at higher altitudes is that of intercepting winds with a higher intensity and, consequently, having a higher energy density.

Reaching winds this high is only possible thanks to flying objects connected to the ground by a cable; this cable can be used to operate a machine that produces electricity or to carry electricity produced on board the aircraft. Of the latter type are some projects that include the drive on board of turbines through the rotation of propellers placed in the wind, while other machines that produce energy on the ground use kite, or textile wings, to be able to unroll the cable. In this way, besides the implicit advantages due to the intercepted wind, the overall dimensions of the machine are reduced compared to what would happen with a turbine and the noise pollution is considerably attenuated. The KITENERGY project stands between these.
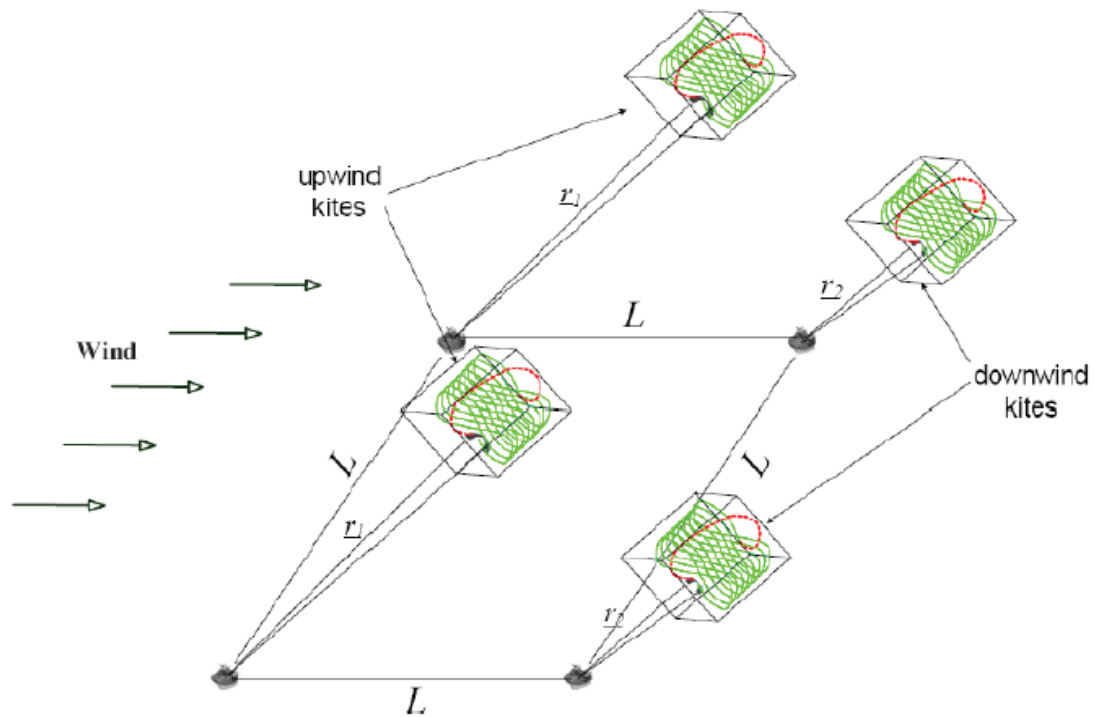
Figure 2.2: Exploitation of high-altitude winds by kite.

Even in the case of high-altitude wind turbines, the idea is to create "farms" capable of producing more power overall; in this case it is necessary to pay attention to the problems deriving from the collision of the systems and the mutual aerodynamic interference.

2.3. The KITENERGY project

Figure 2.3: KITENERGY project.

The KITENERGY is a project that deals with the study and development of an innovative technology for the construction of industrial plants producing electricity from renewable sources.

The underlying idea is the exploitation of high-altitude wind energy captured through a strong and light structure formed by power wing profiles, called Power Kites, which are fixed to pairs of cables made of polymeric material anchored to structures fixed or mobile positioned on the ground. The cables have the dual role of transmitting the traction and simultaneously controlling the flight of the wing profiles.
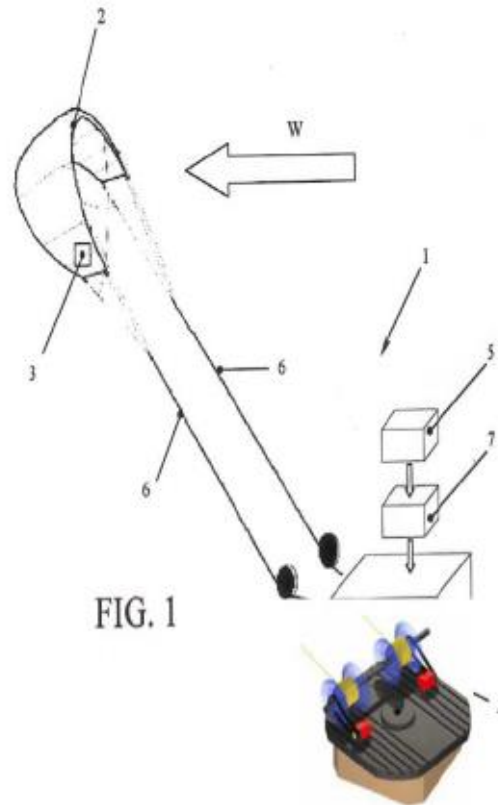
Figure 2.4: KSU (Kite Steering Unit).
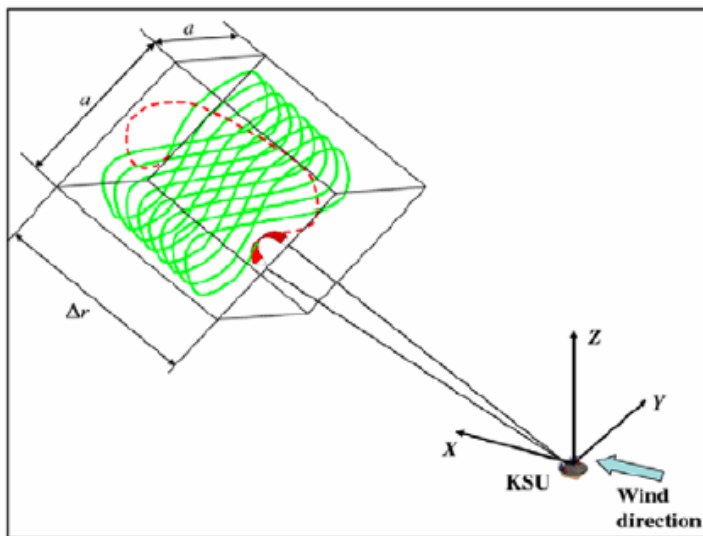
Figure 2.5: Kite manoeuvre.

The essence of the KITENERGY concept is comparable to a wind tower in which only the really necessary components remain, that are the high-speed wings and the generator, this conveniently moved to the ground. The resulting structure, including the ground foundations, is much lighter and cheaper, and allows wind to be captured at altitudes of up to $800 - 1000$ meters. The key technology of the KITENERGY is the KSU, that is the control unit of the power wing profiles (Kite Steering Unit, see

figure 2.5), composed of two electric actuators able to work both as engines and as electric generators. The kite is fixed to a pair of cables, one for each end, and the cables are rolled up to two winches coupled to the actuators. The KSU is also equipped with ground and on-board sensors. The variables that are measured are the wind direction and speed, the coordinates of the wing profile and its speed and acceleration values. Based on the signals obtained from the sensors, the control unit allows to automatically guide the trajectory of the kite through a control unit that maximizes energy generation.

As for the manoeuvre, the kite, deflated and grounded, is pulled by the cables initially so you can start to inflate and then start to develop aerodynamic loads. In this way, the kite can unroll the cables and climb up. The kite, going up, makes eight, in what is called the "generation phase". At the end of it, the kite must be returned to what is called the "recovery phase" in order to rewind the cables. To carry out this manoeuvre, the kite is brought to a position where its aerodynamic resistance is minimal, so as to spend less energy and less time in implementing it. Precisely this manoeuvre represents a major problem in the energy production of an entire cycle (generation and recovery), since it not only requires a waste of energy, but, being slow also to avoid exaggerated requests for power to the system, occupies a considerable time interval of cycle according to the wind speed (from about 20% for light winds, up to 50% for particularly strong winds).

2.4. Aerogenerator for high altitude winds: Fixed wing
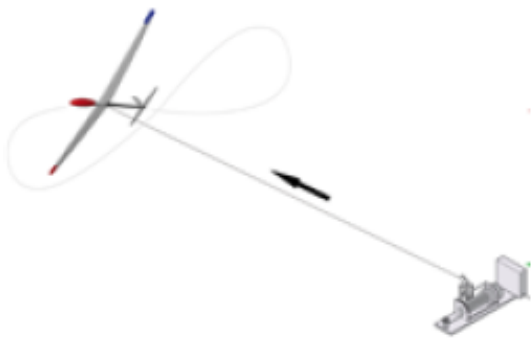
Figure 2.6: Schematization of the system.

The kite used in the KITENERGY project consists of nylon, which allows you to have the best compromise between kite cost, durability and structural strength; higher performance could be achieved using materials used by military parachutes, or for space re-entry, but the cost of the system would be monstrously inflated.

The possibility of using a fixed wing compared to that still used in a textile wing would certainly lead to a generous advantage in the recovery phase, since an aircraft would be orientable to a favourable incidence of a rapid descent and a minimum aerodynamic resistance. What we propose to study with this thesis is the possibility of reaching productions of powers much higher than those that the current system with kite allows (60 kW).

Therefore, a method of calculating the performance of a fixed wing was performed, defined by an aero-structural project, illustrated in the following chapter.

Chapter 3 - Kite definition and requirements

Once the different configurations of wind turbines have been analysed, the KITEnergy project is studied in depth. In this chapter, it will be obtained the shape and dimensions of the studied kite. For this purpose, the previously carried out project is used to estimate the preliminary design of the project.

3.1. Configuration

The 'kite' of the KITEnergy project is not a usual kite. It has the shape of a flying wing but without fuselage, and therefore, has no horizontal stabilizer or vertical stabilizer.

Without the classic elements of stability control, the following two elements are used to perform the same function:

- Elevons: the aircraft has two, one in each wing. They have double function, since if they are activated in the same direction, they exercise the function of the horizontal stabilizer and provide longitudinal control. However, if they are activated in the opposite direction, they fulfil the function of the ailerons.
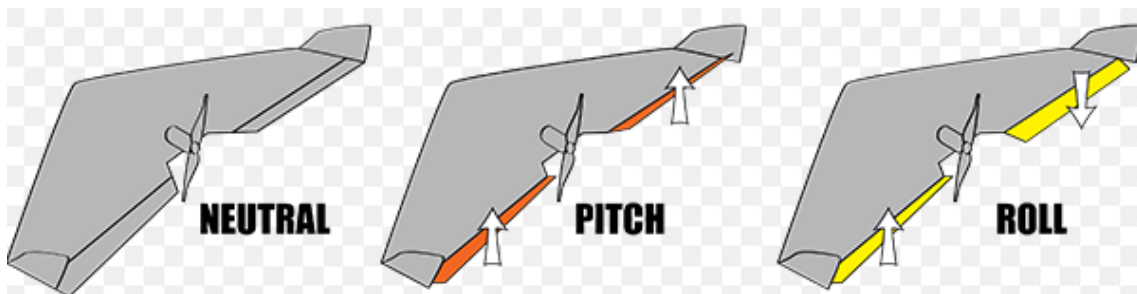
Figure 3.1: Functions of the elevons.

- Rudder at the point of the wing: it has one in each winglet, and fulfils the function of the vertical stabilizer allowing the turn of the aircraft.

Figure 3.2: Rudders in the winglet.

3.2. Dimensions

Once a configuration similar to the flying wing for the kite has been decided, it must be sized. The main geometrical data have been obtained from the thesis " Avamprogetto di un velivolo ad ala fissa per lo sfruttamento dell' energia eolica in quota: analisi aeromeccanica e parametrica/ calcolo aerostrutturale " [3].

3.2.1. Geometric data

The geometric data that describes entirely the kite, are showed in table 3.1:

Table 3.1: Geometric data.

Wingspan	$12\ m$
Root chord c_r	$1.8\ m$
Tip chord c_t	$0.8\ m$
Taper ratio λ	0.44
Standard Mean Chord SMC	$1.3\ m$
Mean Aerodynamic Chord MAC	$1.364\ m$
Wing surface S_w	$15.6\ m^2$
Aspect Ratio AR	9.23
Sweep angle Λ	25°
Aerodynamic centre x_{AC}	$0.6\ m$
Barycentre x_G	$0.7\ m$
Twist angle θ	0°

Knowing the wingspan of the kite and its root chord and tip chord, it is possible to calculate the wing surface assuming that the wing as trapezoidal. It will be necessary for calculating the aerodynamic contributions.

$$S_w = b \cdot SMC = \frac{b^2}{\Lambda} = 15.6\ m^2 \qquad (3.1)$$

where the standard mean chord SMC is obtained from the following equation:

$$SMC = \frac{c_r + c_t}{2} = 1.3\ m \qquad (3.2)$$

Another interesting parameter in the equation 3.1 is the aspect ratio AR, that influence in the structural design of the kite, and its manoeuvrability. As longer is the wing, the wing surface thereof will be bigger, and therefore, the moment created in the wing root (that load it) will increase due to the lift increase. Using the same argument, if the wing is longer, the roll moment created by the elevons increases due to the length increase between the elevon and the wing root. It is defined in equation 3.3:

$$AR = \frac{b}{SMC} = 9.23 \tag{3.3}$$

The fraction between the tip chord c_t and the root chord c_r, is known as taper ratio. It reduces the weight of the wing and the load moment created on the root chord.

$$\lambda = \frac{c_t}{c_r} = 0.44 \tag{3.4}$$

Moreover, the difference between the aerodynamic centre x_{AC} and the barycentre x_G must be known, to calculate the longitudinal stability in fixed commands through the neutral point in fixed commands.

Next, is calculated the mean aerodynamic chord MAC, that is defined as the chord at which the total aerodynamic force can be applied. It must be always greater than the standard mean chord by its definition.

$$MAC = \frac{2}{3}c_r\frac{1 + \lambda + \lambda^2}{1 + \lambda} = 1.364 \, m \tag{3.5}$$

Finally, the sweep angle Λ and the twist angle θ could be studied. The first one gives the proper shape to the wing to avoid the supersonic transient that will not influence in this kite due to its low speed. The other moves the initial stall point towards the centre of the wing, that protects the elevons of the stall at low speed and low angle of attack.

3.2.2. Mass and inertia

To integrate the sum of forces equations, it is necessary to know the mass of the kite, and its inertial moment according to the normal axis ($-y_b$ in body axes). Both are represented in table 3.2:

Table 3.2: Mass and inertia of the kite.

Mass	200 Kg
Moment of inertia I_n	28.8004 $Kg \cdot m^2$

3.2.3. Cable dimensions

The cable must be also dimensioned though its minimum length that indicates the initial point, and its maximum length that set the returning point when a negative command in the seat angle is given.

Table 3.3: Cable length.

Minimum length (m)	Unknown
Maximum length (m)	Unknown

3.2.4. Top view

In the graph below, it can be seen the dimensions aforementioned with a scale 1:25. The elevons and the rudders have also been added to this design, but its dimensions have not been calculated. Those dimensions will be calculated in a next study about the longitudinal stability (elevons sizing), the lateral stability (elevons sizing) and the directional sizing (rudders sizing). The elevons sizing must satisfy both criterions of stability,

0,8 m

1,8 m

12 m

0,7 m

0,6 m

x_{CG} x_{AC}

25°

MAC

SMC
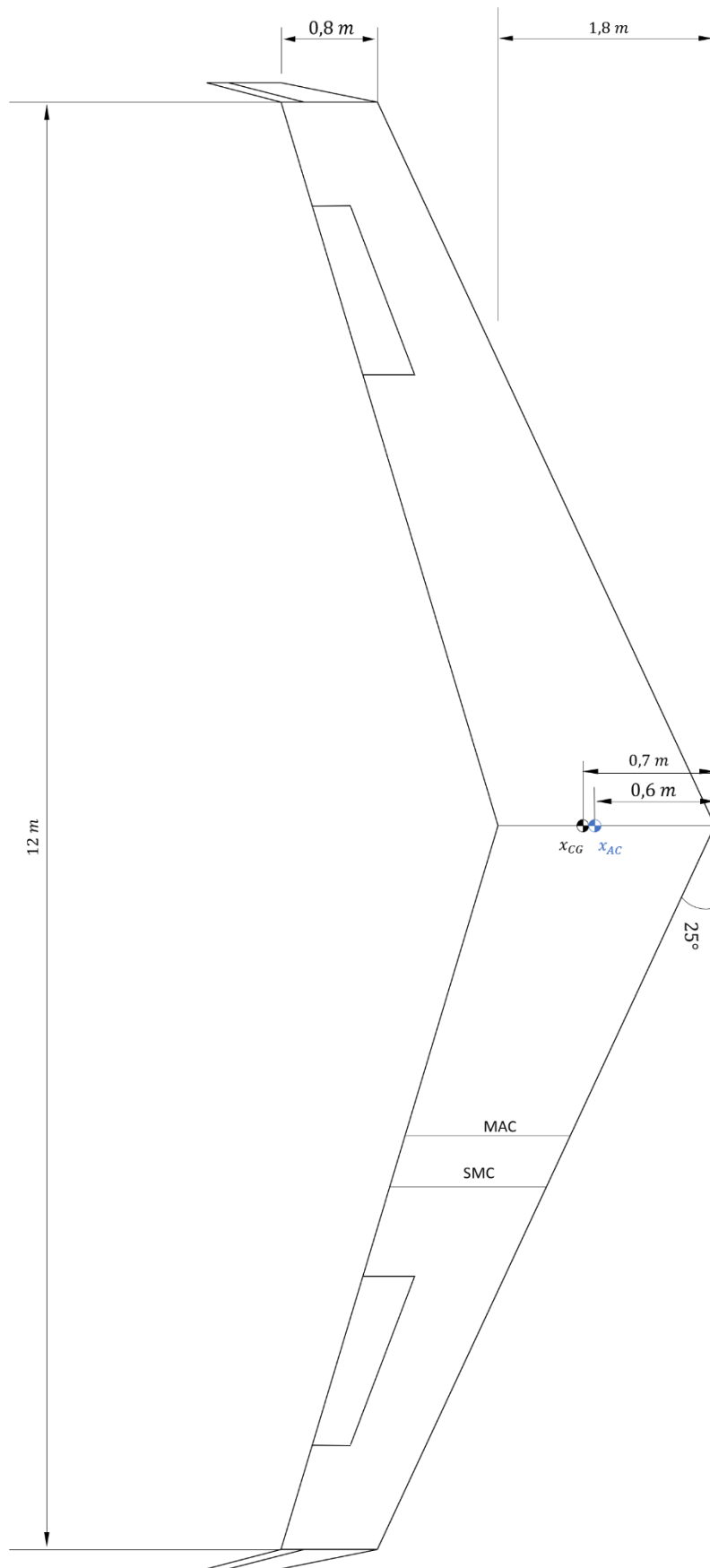
Scale 1:25

Figure 3.3: Top view.

3.3. Hypothesis

The very purpose of this project is to analyse the trajectory of the kite at its design point, neglecting the take-off and landing phases. The kite will always be connected to the ground by a cable, which will be considered fixed in its connection to the ground.

3.3.1. Movement in eight

In the first phase of the project, two types of possible manoeuvre were proposed:

- The circular trajectory: consists of making circles (as its name indicates) at constant height and making a continuous turn around the point of union with the ground.
- The trajectory in eight: it has four different phases:

  1. Phase 1: the first occurs with the wind in favor and moving backwards
  2. Phase 2: in the second one it moves forward with wind against
  3. Phase 3: then, it moves backwards with the wind in favor
  4. Phase 4: finally, it moves forward with wind against again

Between these two movements, it was decided to analyse the second one, because of its greater interest in a later phase of the project. In the next phase, the flight trajectory in crosswind should be analysed.

The two exposed trajectories do not have any interest if they are performed at almost constant height, because they do not produce energy when the cable is not unrolled (the cable does not have a speed of unwinding). But when these same trajectories are studied in crosswind and unwinding the cable (of non-constant height), they can generate a large amount of energy.

From the energetic point of view, it is much more interesting the trajectory in eight, and that is why it has been chosen to analyse its trajectory

For the calculation of the trajectory in eight, several hypotheses and requirements have been imposed:

- The kite is considered in a windy environment, with a wind speed with constant modulus and direction, which has been decided to set at 15 m / s as initial data.
- The movement made by the kite is done at an almost constant height, therefore, it has been decided to consider the seat angle of the speed null.
- The length of the cable that connects the kite to the ground is considered constant.
- Actually, the cable has a winding speed and not constant length, but all this is neglected when considering only the phase of operation at constant height.
- The point of connection between the cable and the kite is made at the centre of gravity of the second, which considerably facilitates the calculation.

Next, the different components of the speed are represented.

$$\vec{V} = \dot{\chi} R \vec{\tau} \qquad (3.6)$$

$$\vec{V_g} = (\dot{\chi} R + V_w \sin \chi)\vec{\tau} + (V_w \cos \chi)\vec{n} \qquad (3.7)$$

$$V^2 = (\dot{\chi}R)^2 \qquad (3.8)$$

As can be seen in Figure 3.4, the kite moves backwards from $\chi = 90°$, due to the component of the wind against it. It also gives the oval shape that is not seen in this schematic figure, but it will be seen in the results chapter.

Finally, it is worth highlighting the angle of sideslip between the aerodynamic speed and its projection in the vertical plane of the kite. This angle is zero in the absence of wind, and is also zero when the kite moves parallel to the wind.
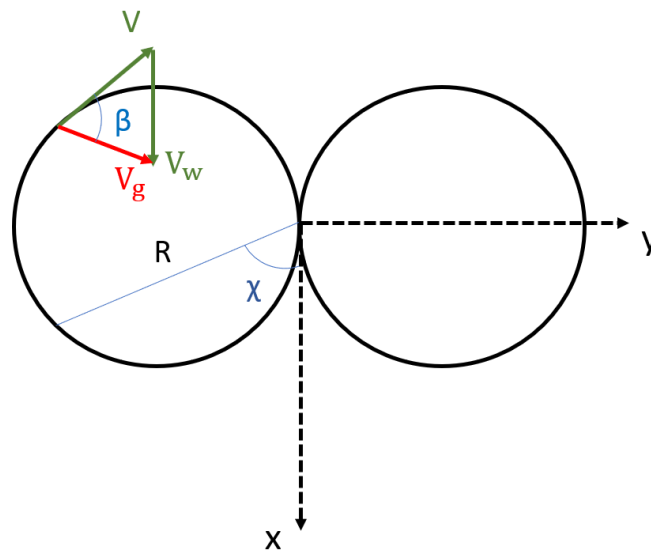

Figure 3.4: Speed decomposition (eight movement) projected in X-Y plane.

3.3.2. Ascending spiral movement

In the second phase of the project, a second trajectory at non-constant height will be studied. As in the first case, the kite will be tied to a cable, but the cable will be unrolled. The movement will consist of two different phases:

- The kite starts an upward movement, making a constant radius turn. When it reaches an angle of rotation $\chi = 180°$, it completely changes its direction to perform the opposite movement. It will never return to its initial position, because it also moves in the direction of the wind, while it is also ascending.
- Once the maximum length of the cable has been reached, a command is given to the elevons to change to a negative seat angle, and thus to return to the starting point of the movement. Likewise, the cable is rolled to recover the initial condition. From this point, the whole process starts over again.

This movement has the following hypothesis:

- The movement is carried out at variable height when unwinding the cable
- The changes of direction every 180º in the angle of rotation are made instantaneously, neglecting the transient
- The climb is made with a constant seat angle during the whole movement, to simplify the problem
- The air density is considered variable by varying the height of flight, the calculation will be made with the ISA atmosphere
- The unwinding speed of the cable is considered constant, because the traction made by the cable is equalised with the aerodynamic forces and the weight in that direction
- The aerodynamic drag and weight of the cable, are considered negligible
- The cable is supposed infinitely rigid, and therefore, it is not broken by traction
- The kite is considered in a windy environment, with a wind speed with constant modulus and direction, which has been decided to set at 10 m / s as initial data
- The turning radius R of the kite is considered constant and of known value, but if the changes of direction were not instantaneous, the turning radius R would increase a little in each transient. This aspect will be the object of study in another project
- The climb to the point of beginning, or the descent are not studied
- The point of connection between the cable and the kite is made at the centre of gravity of the second, which considerably facilitates the calculation
- Losses due to friction between the cable and the bearing on the ground are considered negligible
- The climb is considered the active phase of the movement, because it produces energy, while the descent to the initial point is considered the passive phase because it consumes energy

Chapter 4 - Mathematical model

In this chapter, it will be described the model created to simulate the ascending spiral movement. Once the kite has been described deeply and sized, the relevant simplifying hypotheses were established in the chapter 3.

To implement the model, the tool *'MatLab Simulink'* will be used. Furthermore, the model will be made in a modular way: aerodynamic part, trajectory, speeds, density, angles of positioning, etc.

4.1. Speed calculation

The starting point to create the model, will be to know the desired movement in all its complexity. For this, the first step is to study the speed of the kite.

In figure 4.1, the movement of the kite inside the ascending cylinder is shown, which does not take into account the wind.
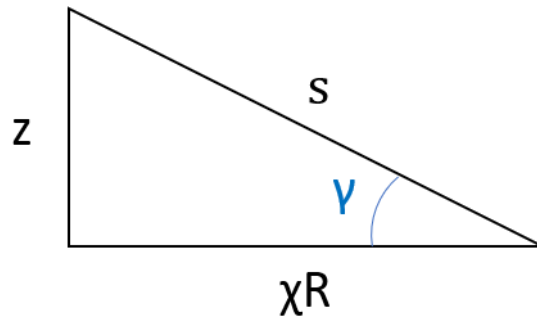

Figure 4.1: Movement inside the ascending cylinder.

where χ is the angle of rotation around the cylinder, z is the ascending coordinate, s is the distance travelled by the kite following its trajectory, R the turn radius, and γ the angle of seat of the speed.

$$s = \frac{\chi R}{\cos \gamma} \tag{4.1}$$

Deriving equation 4.1, the aerodynamic speed is obtained according to its trajectory. Then, the wind speed will be added to obtain the real trajectory of the kite.

$$\vec{V_\tau} = \frac{ds}{dt} = \left[\left(\frac{R}{\cos \gamma} \right) \dot{\chi} + \left(R\dot{\gamma} \frac{\tan \gamma}{\cos \gamma} \right) \chi \right] \vec{\tau} \tag{4.2}$$

$$\vec{V_w} = V_w \vec{\imath} \tag{4.3}$$

The first one, is defined as aerodynamic speed, and the second is the wind speed. The sum of both, defines the speed of the kite with respect to the ground, and therefore, its real trajectory. Likewise, both vectors are represented in XYZ coordinates.

$$\vec{V} = (\dot{\chi}R \cos \chi)\vec{\imath} - (\dot{\chi}R \sin \chi)\vec{\jmath} + \left(\dot{\chi}R \tan \gamma + \chi R \frac{\dot{\gamma}}{\cos^2 \gamma} \right)\vec{k} \qquad (4.4)$$

$$\vec{V_g} = \vec{V} + \vec{V_w} = (\dot{\chi}R \cos \chi + V_w)\vec{\imath} - (\dot{\chi}R \sin \chi)\vec{\jmath} + \left(\dot{\chi}R \tan \gamma + \chi R \frac{\dot{\gamma}}{\cos^2 \gamma} \right)\vec{k} \qquad (4.5)$$

In addition, the square of the aerodynamic speed is calculated, because it will be necessary for obtaining the aerodynamic forces and moments.

$$V^2 = \left[(\dot{\chi}R)^2 + \left(\dot{\chi}R \tan \gamma + \chi R \frac{\dot{\gamma}}{\cos^2 \gamma} \right)^2 \right] \qquad (4.6)$$

4.2. Trajectory calculation

Once the speed of the kite has been obtained, this speed is integrated into its 3 axes to obtain the trajectory, but it should be noticed that the component x and y of the speed change its direction every 180° of the angle of rotation.

$$V_x = V_w \pm \dot{\chi}R \cos \chi \qquad (4.7)$$

$$V_y = \mp \dot{\chi}R \sin \chi \qquad (4.8)$$

$$x = (\pm \dot{\chi}R \cos \chi + V_w)t + x_0 \qquad (4.9)$$

$$y = R \mp (\dot{\chi}R \sin \chi)t \qquad (4.10)$$

$$z = \left(\dot{\chi}R \tan \gamma + \chi R \frac{\dot{\gamma}}{\cos^2 \gamma} \right)t + z_0 \qquad (4.11)$$

In figure 4.2, the speed components are represented in a generic point of the trajectory. Likewise, the aforementioned angle of rotation χ, and also the angle of sideslip β are observed. The angle of sideslip is defined as that formed by the aerodynamic speed and its projection in the vertical plane of the kite.
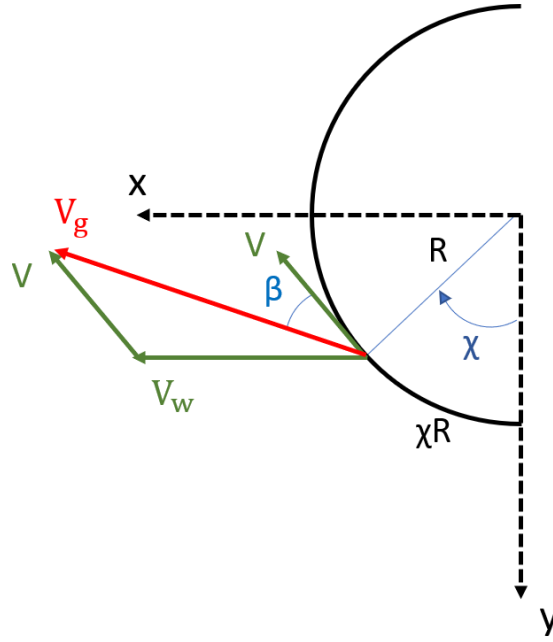
Figure 4.2: Speed decomposition projected in XY plane.

4.3. Angle of sideslip β calculation

To calculate the angle of sideslip, the following vectors should be projected: aerodynamic speed $(\vec{V})$ and speed of the kite $(\overrightarrow{V_g})$. Besides, its modules must be calculated.

$$\overrightarrow{V_{gxy}} = (\dot{\chi}R \cos\chi + V_w)\vec{\imath} - (\dot{\chi}R \sin\chi)\vec{\jmath}$$
$$\overrightarrow{V_{xy}} = (\dot{\chi}R \cos\chi)\vec{\imath} - (\dot{\chi}R \sin\chi)\vec{\jmath}$$

(4.12)

$$\left|\overrightarrow{V_{gxy}}\right| = \sqrt{(\dot{\chi}R)^2 + (V_w)^2 + 2V_w\dot{\chi}R \cos\chi}$$
$$\left|\overrightarrow{V_{xy}}\right| = \dot{\chi}R$$

(4.13)

Knowing these vectors, the angle of sideslip β is obtained from the scalar product thereof.

$$\overrightarrow{V_{gxy}} \cdot \overrightarrow{V_{xy}} = (\dot{\chi}R)^2 + V_w\dot{\chi}R \cos\chi = \left|\overrightarrow{V_g}\right| \cdot \left|\vec{V}\right| \cos\beta$$

(4.14)

4.4. Angle of the cylinder axis ε calculation

Knowing the coordinates x and z of the kite, the angle of the cylinder axis (ε) is calculated as follows:
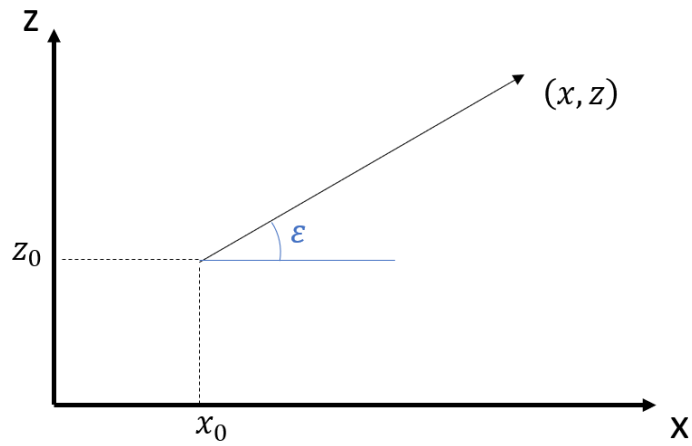
$$\tan\varepsilon = \frac{z - z_0}{x - x_0}$$

(4.15)

Figure 4.3: Angle of the cylinder axis.

4.5. Sum of forces and moments

Having defined the trajectory and the speed in its totality, the next step will be to formulate the sum of forces and moments. To do this, the forces involved in the kite are represented graphically in figures 4.4 and 4.5.
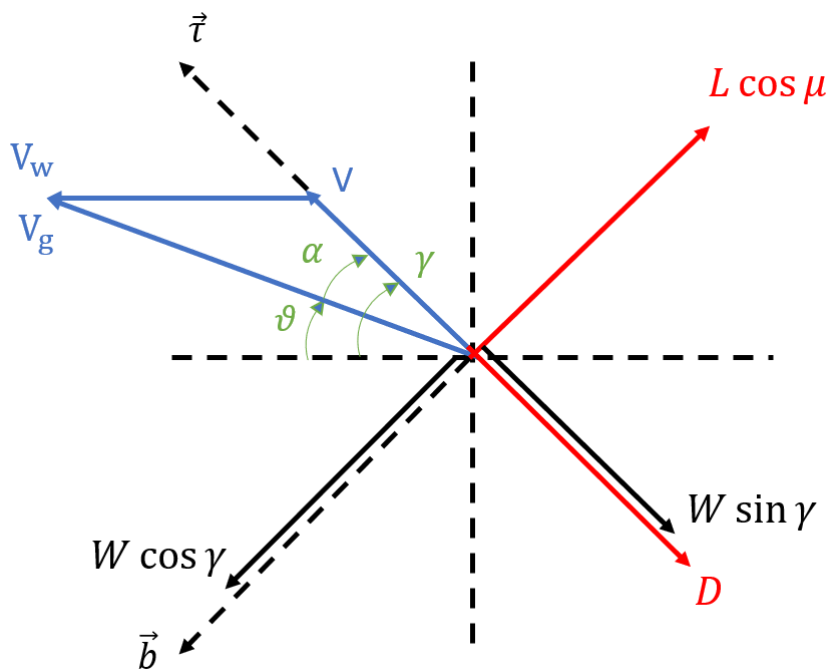

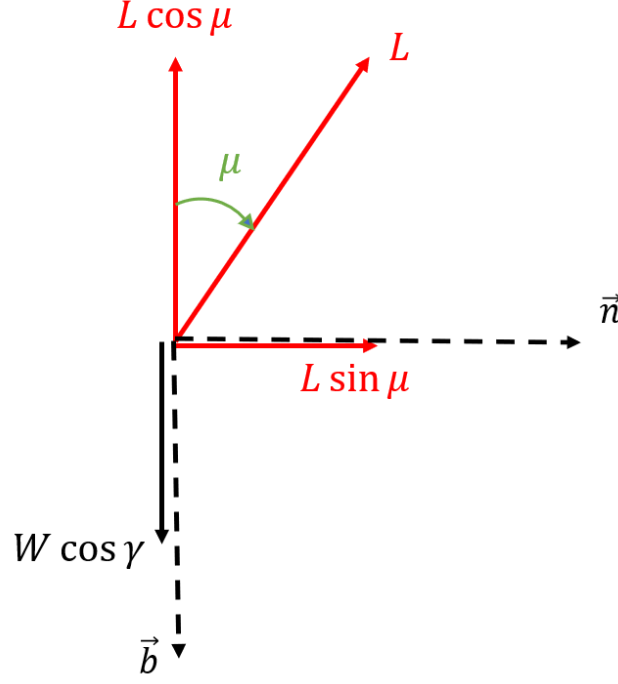Figure 4.4: Force components and speeds in τ-b plane.

Figure 4.5: Force components and speeds in n-b plane.

where ϑ is the angle of seat, α is the angle of attack, γ is the angle of seat of speed, μ is the roll angle, W is the weight of the kite, L is the lift, and D is the drag of the kite.

In equations 4.16 and 4.17, the sum of forces is calculated according to the tangential and normal axes, respectively. This coordinate system is known as wind axes, because the tangential axis follows the aerodynamic speed.

$$\sum F_\tau = ma_\tau \quad \rightarrow \quad -D - W\sin\gamma = ma_\tau \tag{4.16}$$

$$\sum F_n = ma_n = m\frac{(V_{\perp n \in XY})^2}{R} \quad \rightarrow \quad L\sin\mu = m\frac{(V_{\perp n \in XY})^2}{R} \tag{4.17}$$

To solve the equation 4.16, it is necessary to know the tangential acceleration of the kite, for which, the equation 4.2 previously calculated is derived.

$$a_\tau = \frac{dV_\tau}{dt} = \left(\frac{R}{\cos\gamma}\right)\ddot{\chi} + \left(2R\dot{\gamma}\frac{\tan\gamma}{\cos\gamma}\right)\dot{\chi} + \left(R\ddot{\gamma}\frac{\tan\gamma}{\cos\gamma} + R\dot{\gamma}\frac{1 + \sin^2\gamma}{\cos^3\gamma}\right)\chi \tag{4.18}$$

Therefore, the angle of rotation χ of the kite is obtained by integrating the sum of forces equation along the tangential axis.

To solve equation 4.17, it is necessary to know the velocity perpendicular to the normal axis and contained in the XY plane. Consequently, from this equation the roll angle is obtained.

$$V_{\perp n \in XY} = \dot{\chi} R + V_w \cos \chi \qquad (4.19)$$

Finally, the angle of attack α of the kite is calculated by summing the moments according to the normal axis. To do this, the forces and moments necessary for the calculation of said angle are represented in the figure 4.6.
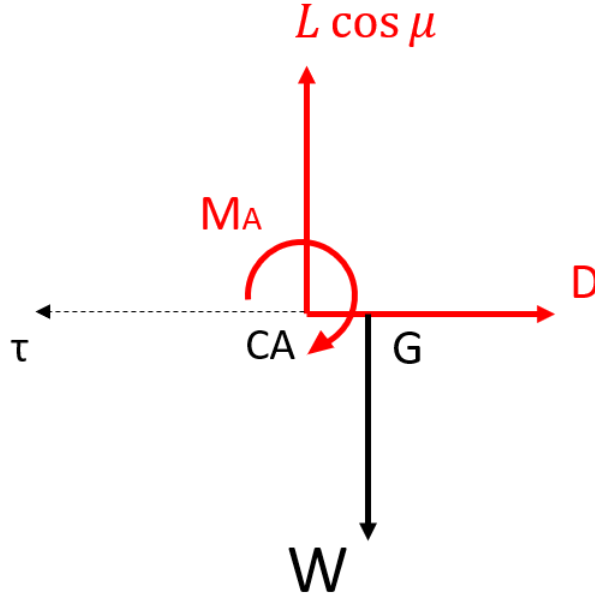

Figure 4.6: Force and moment components in τ -z plane.

In equation 4.22, the sum of moments is formulated at the centre of gravity of the kite. The aerodynamic centre, the centre of gravity and the corresponding moment of inertia are required in this equation, which were obtained in chapter 3.

$$\sum M_\vartheta = I_y \ddot{\alpha} \quad \rightarrow \quad M_{ca} + L \cos \mu \, (x_{cg} - x_{ca}) = I_y \ddot{\alpha} \qquad (4.22)$$

In figure 4.6, it is also observed that aerodynamic drag and weight cannot create moment in the centre of gravity of the kite, since they pass through it.

Moreover, care should be taken with the position of the centre of gravity and aerodynamic centre, since they vary the neutral point in fixed commands of the kite. The neutral point in fixed commands is defined as the position of the centre of gravity that cancels $C_{m\alpha}$, and therefore fixes the longitudinal stability limit.

As it is observed, in this model the aerodynamic forces and moments are present, and therefore, it is necessary to know the square of the aerodynamic speed (V^2) and the density of the air in the height of flight. The first one is obtained from equation 4.6, and the second is defined below.

4.6. Density calculation (ISA atmosphere)

To obtain the flight density, the ISA (International Standard Atmosphere) atmosphere is used as a function of the flight height.

$$T(h) = T_0 + a(h - h_0) \tag{4.20}$$

$$\rho(h) = \rho_0 \left(\frac{T(h)}{T_0}\right)^{\frac{-g}{aR}-1} \tag{4.21}$$

where the data with subscript 0 are referred to sea level, the parameter a is the temperature gradient in the troposphere, g the gravity acceleration, and R the universal constant of ideal gases.

Table 4.1: ISA atmosphere data.

$T_0(K)$	288.15
$h_0(m)$	0
$\rho_0(kg/m^3)$	1.225
$a(K/m)$	$-6.5 \cdot 10^{-3}$
$R(m^2/s^2 K)$	287
$g(m/s^2)$	9.80665

4.7. Angle of seat of speed γ calculation

To close the angular positioning, a seat angle ϑ is imposed to calculate the seat angle of the speed γ in the equation 4.23.

$$\vartheta = 15°$$

$$\vartheta = \alpha + \gamma \tag{4.23}$$

$$\dot{\gamma} = -\dot{\alpha} \tag{4.24}$$

The fixed seat angle aforementioned can be replaced by another value according interest.

4.8. Aerodynamic analysis

The aerodynamic contributions together with the tension exerted by the cable, generate the accelerations that drive the movement of the kite. For the analysis of aerodynamic contributions, it is necessary to calculate the aerodynamic coefficients of the kite. To do this, the 2D analysis of the aerodynamic airfoil must be performed, and then the 3D analysis of the joint wing.

4.8.1. Aerodynamic coefficients calculation

4.8.1.1.　　2D analysis

For the 2D aerodynamic study, the 'Xfoil' tool has been used. This tool allows the obtaining of the coefficients of an aerodynamic profile from its code NACAXXXX, whose numbers indicate:

- The first digit describe the maximum camber as percentage of the chord
- The second digit describe the distance of maximum camber from the airfoil leading edge in tens of percent of the chord
- The last two digits describe the maximum thickness of the airfoil as percent of the chord

Likewise, it allows to realize studies in viscous or non-viscous regime, as well as it allows to vary the number of Reynolds.
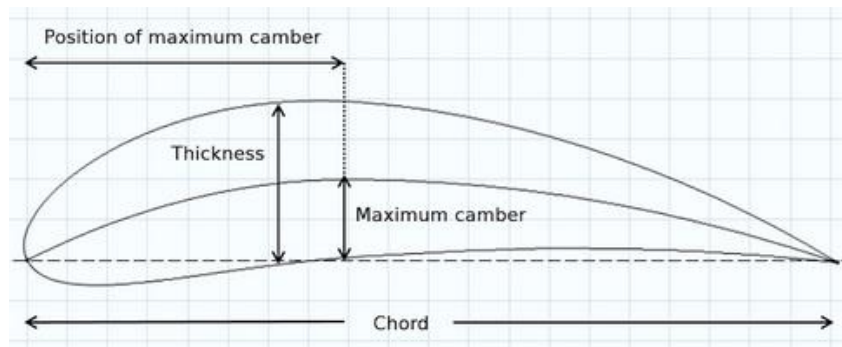

Figure 4.7: NACA airfoil.

4.8.1.2.　　3D analysis

For 3D aerodynamic study, all sections of the kite should be integrated along the wing. Based on the data obtained from the NACA airfoil, the Prandtl lifting-line theory is applied for its integration.
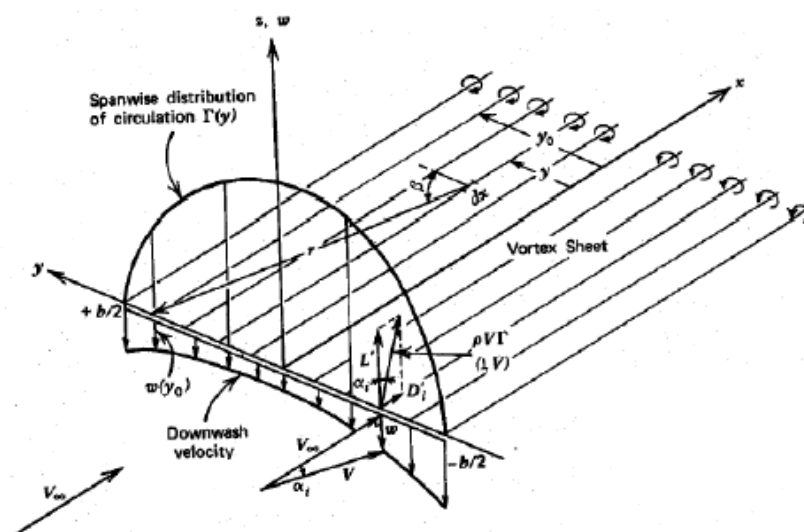

Figure 4.8: Prandtl lifting-line theory.

In this project the Prandtl theory is not explained, because it is not the purpose of it. Therefore, the data is obtained from a previous project that made such calculations.

Table 4.2: Aerodynamic coefficients.

C_{L0}	0.7
$C_{L\alpha}$	4.398
C_{d0}	0.02
C_{m0}	0.01
$C_{m\alpha}$	−1.4
$C_{m\delta e}$	Unknown

With all this, the total aerodynamic characteristics of the wing are obtained, being able to draw its polar.

$$C_L = C_{L0} + C_{L\alpha}\alpha \tag{4.25}$$

$$C_D = C_{d0} + \frac{C_L^2}{\pi Ae} \tag{4.26}$$

$$C_{mca} = C_{m0} + C_{m\alpha}\alpha + C_{m\delta e}\delta_e \tag{4.27}$$

These three aerodynamic coefficients will be strongly linked to the angle of attack of the kite, which has been calculated in this chapter. Finally, it should be noted the dependence of the moment coefficient with the angle of deflection of the elevon, which will be used later to perform the longitudinal control.

For the calculation of the lift, the drag and the aerodynamic moment, it is necessary to know the density in which the kite flies, and its aerodynamic speed.

4.8.2. Aerodynamic forces and moments

Once the aerodynamic coefficients, the density and the aerodynamic speed have been obtained, the lift, drag and the aerodynamic moment are calculated.

$$L = \frac{1}{2}\rho SV^2 C_L \tag{4.28}$$

$$D = \frac{1}{2}\rho SV^2 C_D \tag{4.29}$$

$$M_{ac} = \frac{1}{2}\rho cSV^2 C_{mac} \tag{4.30}$$

4.9. Cable traction

As it was said in the hypothesis chapter, the traction executed by the cable will be an opposite force that reacts to the force created by the kite in the cable direction, which includes the lift, the aerodynamic drag and its weight. The first step will be to decompose the aforementioned forces in the ground system (XYZ):

$$\vec{W} = -W\vec{k} \tag{4.31}$$

$$\vec{L} = -L(\cos\mu\sin\gamma\cos\chi + \sin\mu\sin\chi)\vec{i} + \\ +L(\cos\mu\sin\gamma\sin\chi - \sin\mu\cos\chi)\vec{j} + L\cos\mu\cos\gamma\,\vec{k} \tag{4.32}$$

$$\vec{D} = -D(\cos\gamma\cos\chi)\vec{i} + D(\cos\gamma\sin\chi)\vec{j} - D\sin\gamma\,\vec{k} \tag{4.33}$$

Then, those force are summed to obtain the total force that influence in the kite:

$$\vec{F} = \vec{L} + \vec{D} + \vec{W} \tag{4.34}$$

Knowing the position of the kite $\vec{s}$, it is defined the normalized vector $\vec{u_s}$ (versor) that indicates the kite direction any time as follows, as seen in figure 4.9:
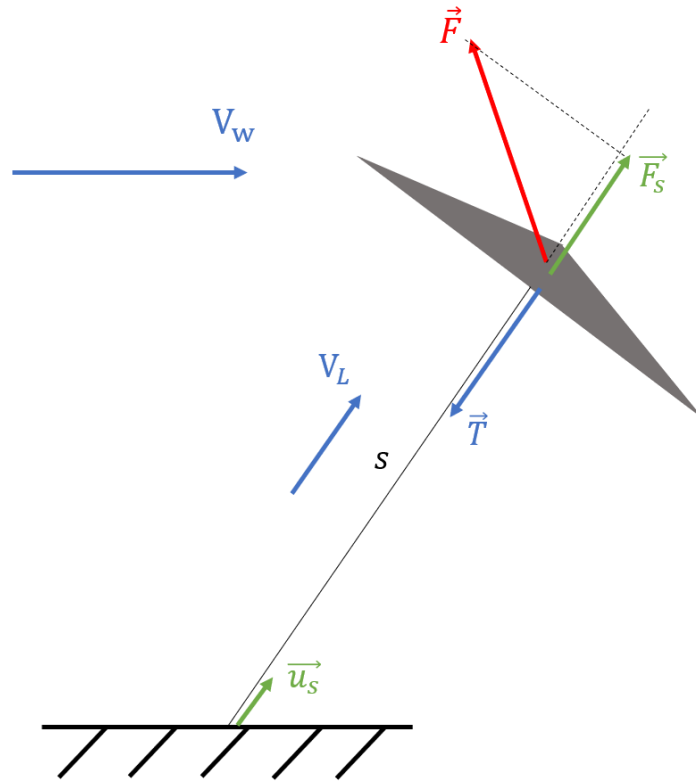

Figure 4.9: Total force projection.

$$\vec{s} = x\vec{i} + y\vec{j} + z\vec{k} \tag{4.35}$$

$$\vec{u_s} = \frac{\vec{s}}{|s|} \tag{4.36}$$

Afterwards, the total force executed by the kite is projected on the direction of the kite $\vec{u_s}$ to obtain the traction developed by the cable:

$$F_s = \vec{F} \cdot \vec{u_s} = T \tag{4.37}$$

4.10. Active power

To close the model, the active power created by the kite is obtained through the equation 4.38, that involves the traction and the unwinding speed.

$$P_a = V_l \cdot |F_s| \tag{4.38}$$

This active power should be integrated with the time to obtain the total energy obtained in the ascending movement. It will be integrated by the trapezoidal rule, using the command *trapz*. In a next study, the passive power consumed in the descending movement should be calculated, which will be used to calculate the available power, that is defined as the difference between both powers.

Chapter 5 - Code manual

In this this chapter will be explained a tutorial to use the model of the kite. It has been designed as a modular model with several inputs and outputs in each module. The first step to run the trajectory model, is the data definition of the problem that will be introduced in the script '*Main.m*'. Some general data are shown in figure 5.1:

```
m = 200;                % Mass of the kite (Kg)
g = 9.80665;            % Constant of gravity (m/s^2)
w = 0.25;               % Angular frequency (rad/s)
R = 70;                 % Turn ratius (m)
theta = 15;             % Seat angle (°)

Vw = 8;                 % Wind speed (m/s)
Vl = Vw/3;              % Unwinding speed (m/s)
```

Figure 5.1: General data.

At this point, the constant data commented in the hypothesis have been fixed, and some other data as the mass of the kite, or its moment of inertia according to the normal axis are also introduced. Besides, it is assumed that the unwinding speed is the third part of the wind speed.

$$V_l = \frac{V_w}{3} = cte \tag{5.1}$$

Then, the geometric data that define the shape of the kite are introduced in the following section of the script.

```
cr = 1.8;                                        % Root chord (m)
ct = 0.8;                                        % Tip chord (m)
b = 12;                                          % Wingspan (m)
lambda = ct/cr;                                  % Taper ratio
SMC = (cr+ct)/2;                                 % Standard Mean Chord (m)
MAC = 2/3*cr*(1+lambda+(lambda^2))/(1+lambda);   % Mean Aerodynamic Chord (m)
Sw = 2*SMC*(b/2);                                % Wing surface (m^2)
AR = b/SMC;                                      % Aspect ratio
e = 0.9;                                         % Oswald factor

xcg = 0.7;                                       % Barycentre (m)
xac = 0.6;                                       % Aerodynamic centre (m)
```

Figure 5.2: Geometric data.

The shape and the dimensions of the kite can be changed in this section, but it should be taken into account that some values entail complex results in some subsequent calculation, therefore cannot be introduced very strange dimensions.

The last data introduced in the script are the corresponding to the aerodynamic coefficients. In figure 5.3 are presented the several coefficients.

```
%% Aerodynamic coefficients

Cl0 = 0.7;                      % Lift coefficient Cl0
Clalpha = 2*pi;                 % Lift coefficient Clalpha
Cd0 = 0.02;                     % Drag coefficient Cd0
Cmo = 0.01;                     % Aerodynamic moment coefficient Cm0
Cmalpha = -1.4;                 % Aerodynamic moment coefficient Cmalpha
```

Figure 5.3: Aerodynamic coefficients.

All this data previously introduced will be read by the Simulink file '*ascendinghelix.slx*' before the simulation. Moreover, the simulation time and the fixed time step used to integrate the model must be chosen. The choice of the fixed time step is very interesting, because as smaller is the step, more refined will be the simulation, but it has the disadvantage of the computational cost that increases with the reduction of the step.

```
%%%%%%%%%%%%%%%%%%%%%%%%%%%%%%%%%%%%%%%%%%%%%%%%%%%%
%%%%%%%%%% SIMULINK MODEL MUST BE RUN %%%%%%%%%%
%%%%%%%%%%%%%%%%%%%%%%%%%%%%%%%%%%%%%%%%%%%%%%%%%%%%

t_simulation = 180;             % Simulation time introduced in s
t_step = 0.01;                  % Fixed time step introduced in s

sim('ascendinghelix');

t = tout;
```

Figure 5.4: Simulation time specification.

Once all the data have been chosen, the Simulink model must be run externally with the MatLab command *sim ('name of the model')*. The data could be introduced as a number inside the model, but it would be more confusing for the user. The model can also be run inside the '*Simulink model*'.

Finally, there are some graphs (for the results chapter) specifications using code LaTex in its labels, as the following example:

```
% Aerodynamic Speed (m/s)

figure(2)
plot(t,ChidotR)
grid
xlabel('time (s)','interpreter','latex')
ylabel('$\stackrel{.}{\chi}$R (m/s)','interpreter','latex')
```

Figure 5.5: Graph specification example.

In the last section of the script, the total active energy created by the kite is obtained from the active power evolution with the time though the Matlab command *trapz (time step, function)*. Where the first parameter is the time step previously chosen, and the second parameter is the active power evolution with time.

```matlab
Paverg = mean(Active_Power);                    % in W
Eactive = trapz(t_step,Active_Power)/(3.6e6);   % in Kwh
```

Figure 5.6: Power integration

Chapter 6 - Results

In this chapter, the results obtained from the model made in chapter 4 will be studied. It will start by calculating the flight characteristics that will be called nominal, because they will define the nominal movement of the kite. The same solution path previously proposed in the model will be followed.

Then, a study of the power produced by the kite (climb movement) is developed. The difference between this power and the power consumed in the descent will be the available power of the kite in its movement. It will be completed by carrying out a study varying the intensity of the wind speed.

6.1. Nominal case

6.1.1. Speed results

First, the speed of the kite is calculated in its different variants (wind speed, aerodynamic speed and speed of the kite).

Figure 6.1 shows the nominal value of the wind speed. As had been mentioned before, a constant value has been established throughout the trajectory as a hypothesis of the problem. Taking into account the typical values of the wind in this region, the following value has been decided:

$$V_w = 10 \ m/s \tag{6.1}$$
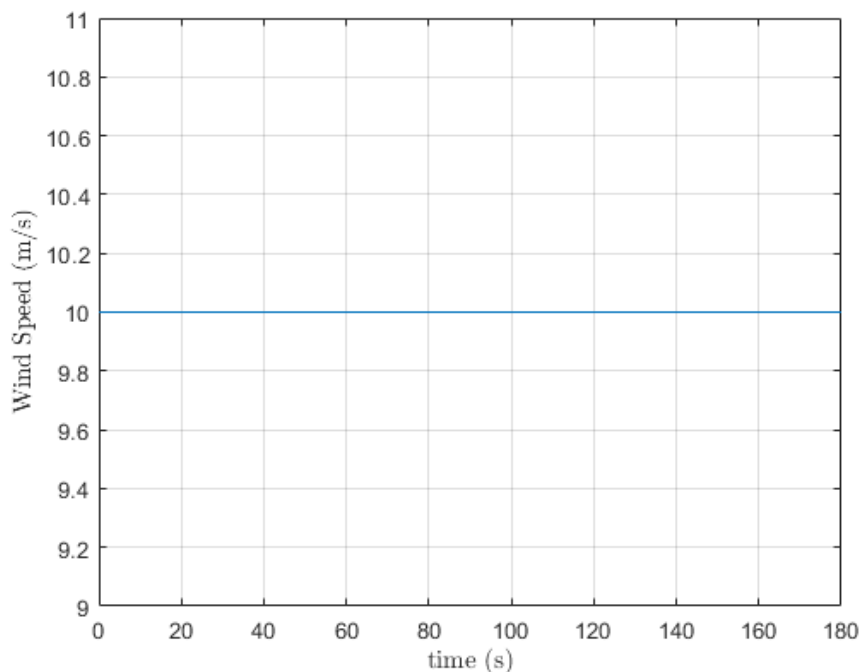
Figure 6.1: Wind speed against time.

The aerodynamic speed of the kite depends on the angular speed $\dot{\chi}$ and the turning radius R, therefore, it is variable with time. The angular speed $\dot{\chi}$ will be positive when the angle of rotation χ varies between 0° and 180°, and negative when the angle of rotation χ decreases between 180° and 0°. In the first interval, its value varies between $0\ rad/s$ and $0.5\ rad/s$, with an average value of $0.25\ rad/s$, while in the second, it varies between $-0.5\ rad/s$ and $0\ rad/s$, with an average value $-0.25\ rad/s$. To summarize, the angular velocity varies as follows:

$$\begin{cases} \dot{\chi} \in [0\ rad/s, 0.5\ rad/s] & if \quad \chi \in [0\,°, 180°] \quad with \quad \dfrac{d\chi}{dt} > 0 \\ \dot{\chi} \in [-0.5\ rad/s, 0\ rad/s] & if \quad \chi \in [180\,°, 0°] \quad with \quad \dfrac{d\chi}{dt} < 0 \end{cases} \tag{6.2}$$

However, the turning radius R will have a constant value throughout the trajectory. Its nominal value will be:

$$R = 70\ m \tag{6.3}$$

In figure 6.2, it is observed that the aerodynamic speed trend is similar to the angular speed. In equation 4.2, the two terms of said speed are observed. The first one is almost the angular velocity $\dot{\chi}$ scaled with the turning radius R (because the γ angle is very small, and therefore, its cosine is almost 1), while the second term represents the ascensional speed that is much smaller than the first one.
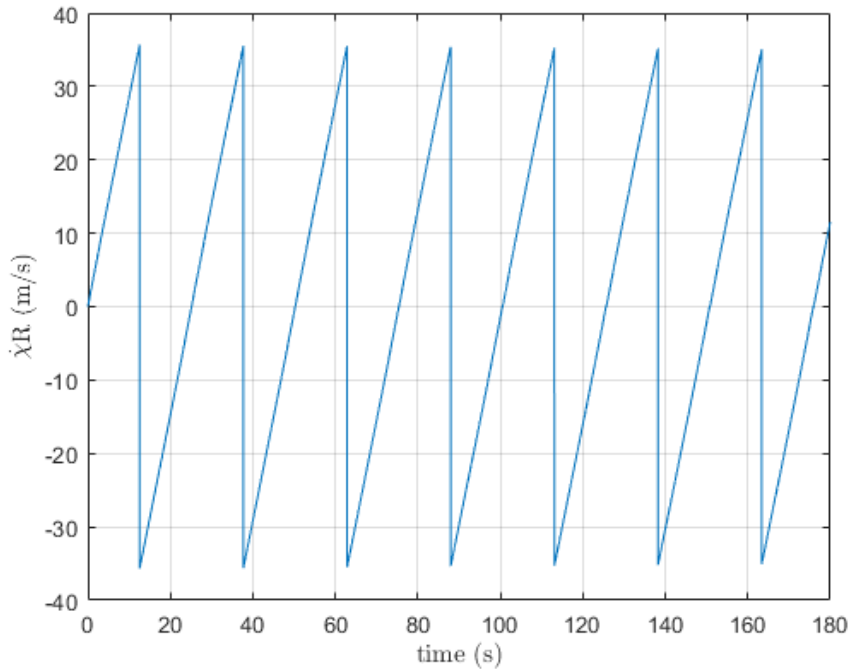

Figure 6.2:Aerodynamic speed against time.

Knowing the average angular velocity $\dot\chi = 0.25\ rad/s$ in absolute value and that the change of direction occurs at $180°$, it can be calculated in which second the change of direction will take place.

$$t_{change} = \frac{\chi_{change}}{|\dot\chi_{average}|} = \frac{180°}{0.25\ rad/s}\frac{2\pi\ rad}{360°} = 12.566\ s \tag{6.4}$$

Then, the overall speed of the kite $\vec{V_g}$ respect to the ground is obtained. From equation 4.5, it is observed that it is obtained as the vector sum of the aerodynamic speed $\vec{V}$ and the wind speed $\vec{V_w}$. In figures 6.3, 6.4 and 6.5, the speed of the kite is represented according to the axes X, Y and Z.

In the component x of the velocity V_x, it is observed how it decreases (being even negative at low wind speed) when the angle of rotation χ increases, due to the great influence of the $\cos\chi$ (see equation 4.7). Furthermore, the contribution of the aerodynamic speed changes its sign when it reaches $180°$, because the kite changes its direction instantaneously (hypothesis of the problem). However, the contribution of wind speed remains constant throughout the movement.
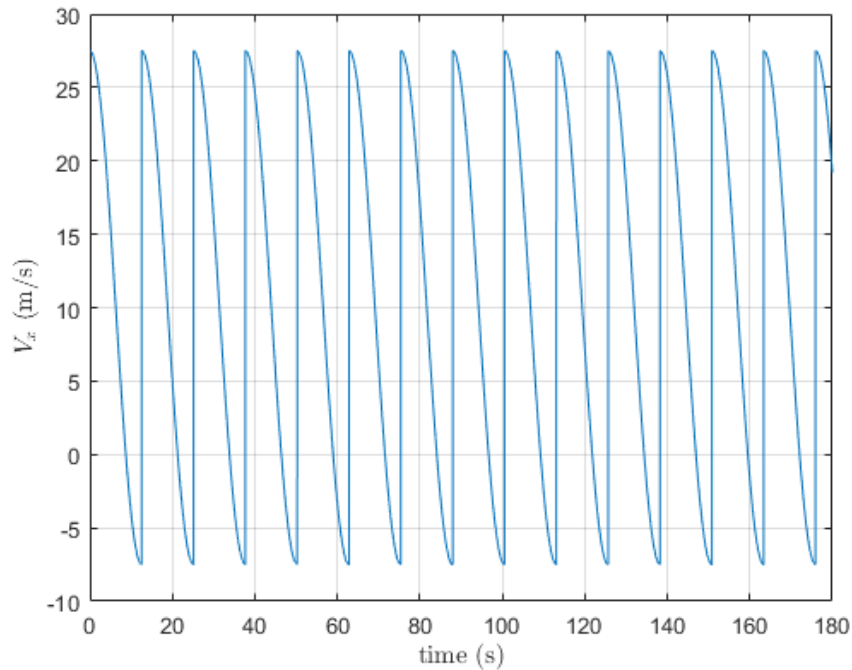

Figure 6.3: V_x speed component against time.

The component V_y of the speed of the kite is a sinusoidal response as shown in equation 4.8, and always reaches its maximum in absolute value in $\chi = 90°$. Besides, it is observed as negative in the first interval defined in equation 6.2, and positive in the second interval. These two intervals of results for V_x and V_y are repeated every $360°$.
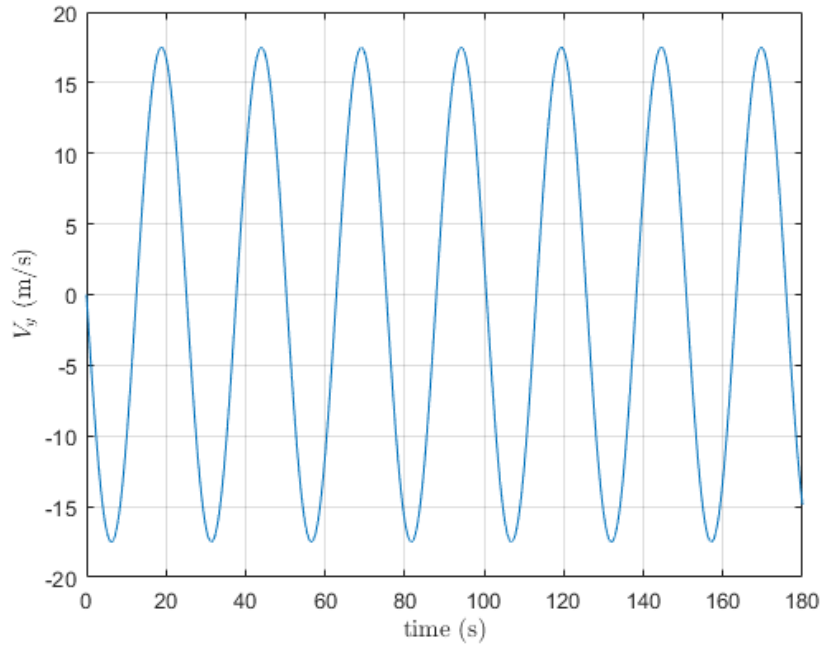
Figure 6.4: V_y speed component against time.

The component V_z of the speed of the kite is obtained from equation 4.5. Its absolute value is less than the two previous components, being V_x the largest because of the contribution of the wind speed, and V_y the intermediate one. This component also has two contributions, the first is small because γ is small (tan γ is small), and the second is greater, but not as much as V_x and V_y. This climbing speed has a strange shape, because it depends on a large amount of non-constant variables (γ, $\dot{\gamma}$, χ and $\dot{\chi}$). It also has a fast transient that evolve in a periodic speed.
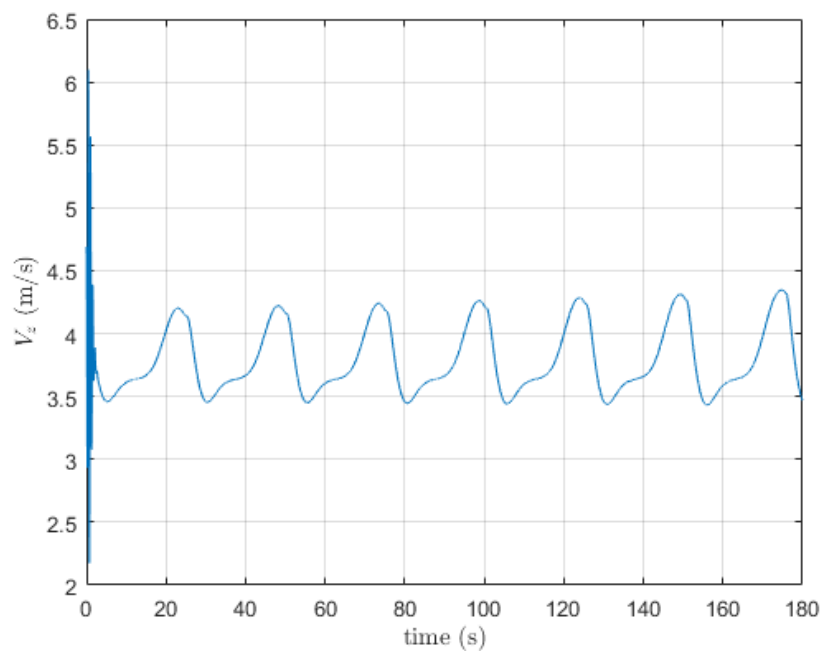
Figure 6.5: V_z speed component against time.

To finish the section of the speeds of the kite, the square of the aerodynamic speed V^2 is shown in figure 6.6. A trend similar to V_z is observed, but increased with $\dot{\chi}R$ and squared. This speed squared calculated in the equation 4.6, is necessary for the later calculation of the aerodynamic components (lift L, aerodynamic drag D and aerodynamic moment M_{ac}). It has the same initial transient that evolve quickly in a periodic speed.
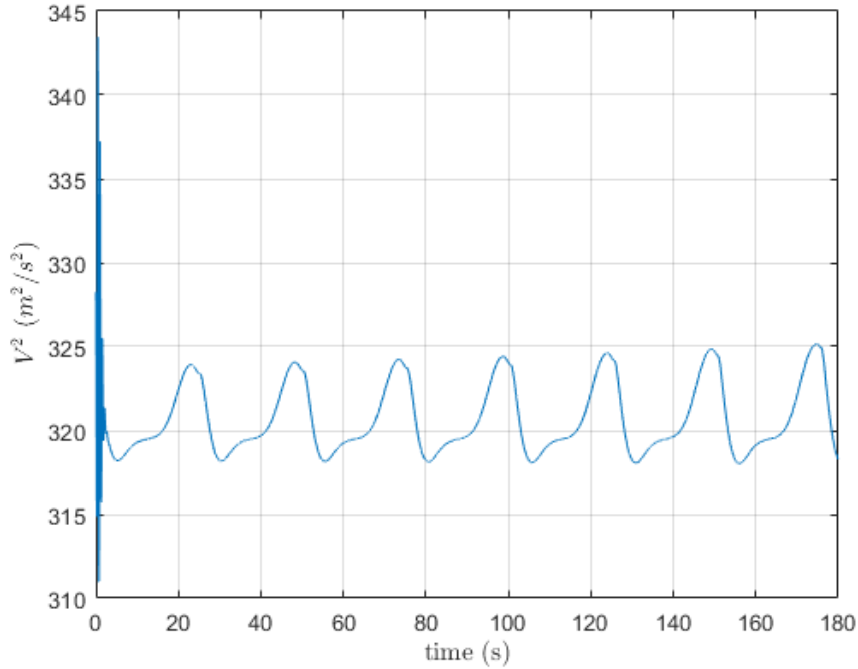

Figure 6.6: Aerodynamic speed squared V^2.

6.1.2. Trajectory results

Once the calculation of the different speeds of the kite has been completed, the speeds of the kite with respect to ground are integrated in the 3 axes. In addition, initial conditions must be imposed to initiate the movement of the kite. The following initial conditions may be changed in a subsequent analysis.

$$(x_0, y_0, z_0) = (40\ m, R, 80\ m) \tag{6.5}$$

In figure 6.7, the evolution of the coordinate x as a function of time is represented. In this figure, it is observed the previously marked initial point, as well as its slightly sinusoidal evolution by its own definition in the equation 4.9. Another remarkable aspect is its greater growth with respect to the other coordinates, because the wind speed V_w has the direction of the X axis.
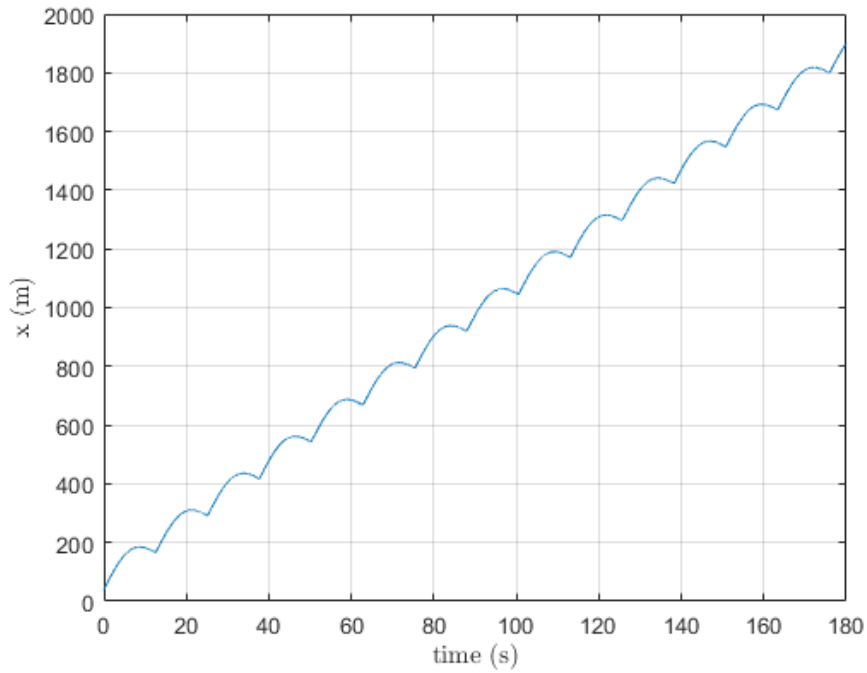
49

Figure 6.7: Coordinate x of the kite against time.

In figure 6.8, the evolution of the coordinate y of the kite as a function of time is observed. As shown in equation 4.10, it has a sinusoidal shape and changes its sign when it reaches the angle of rotation $\chi = 90°$. In order to achieve an ascending cylinder of constant radius R, an initial condition equal to the turning radius R must be set, between whose values the y coordinate varies.
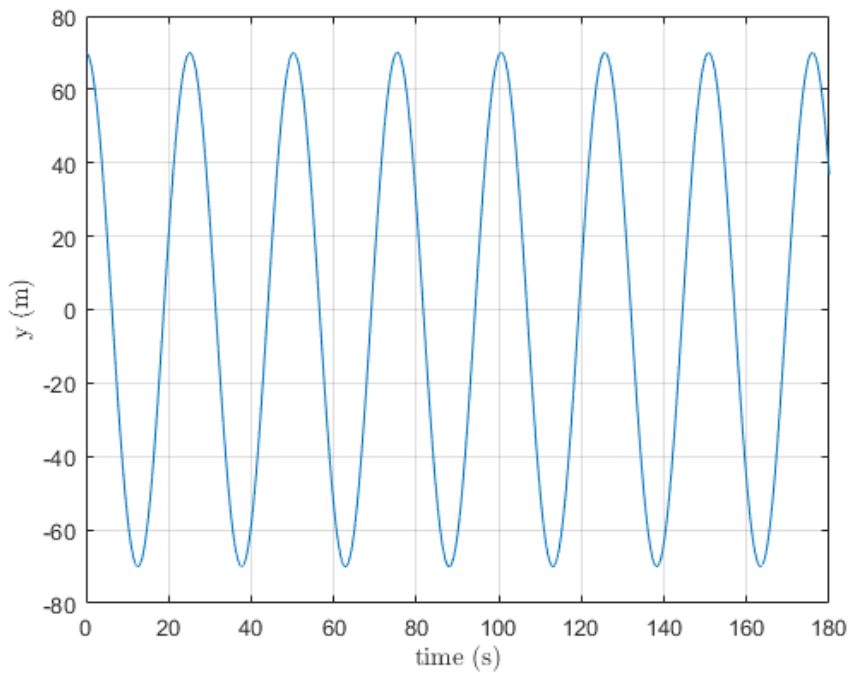

.

Figure 6.8: Coordinate y of the kite against time.

The last coordinate to be analysed will be the ascending z, which starts its travel in the initial condition previously set. Its growth is less than the x coordinate as expected, and its shape is collected in equation 4.11. It is represented in figure 6.9.
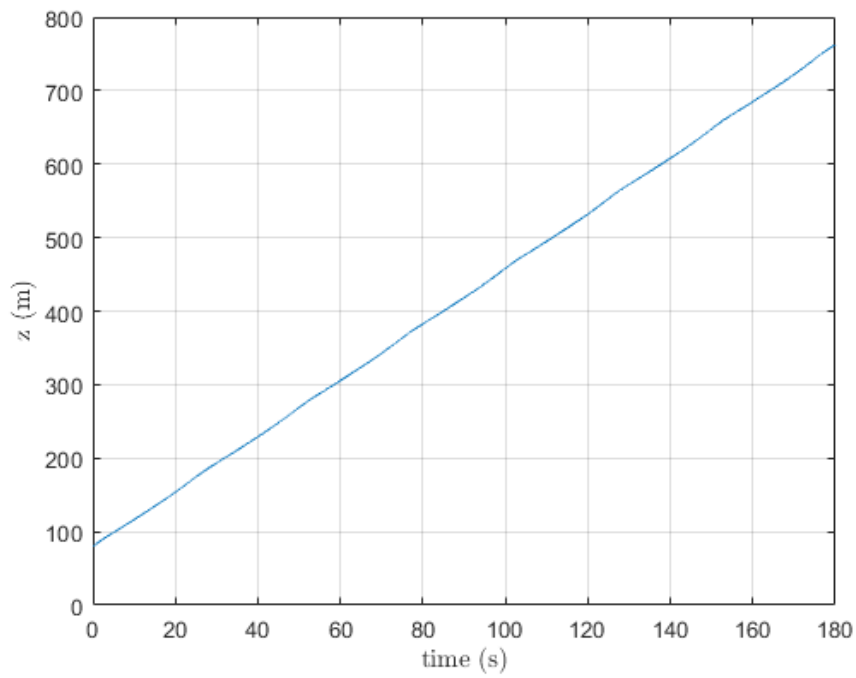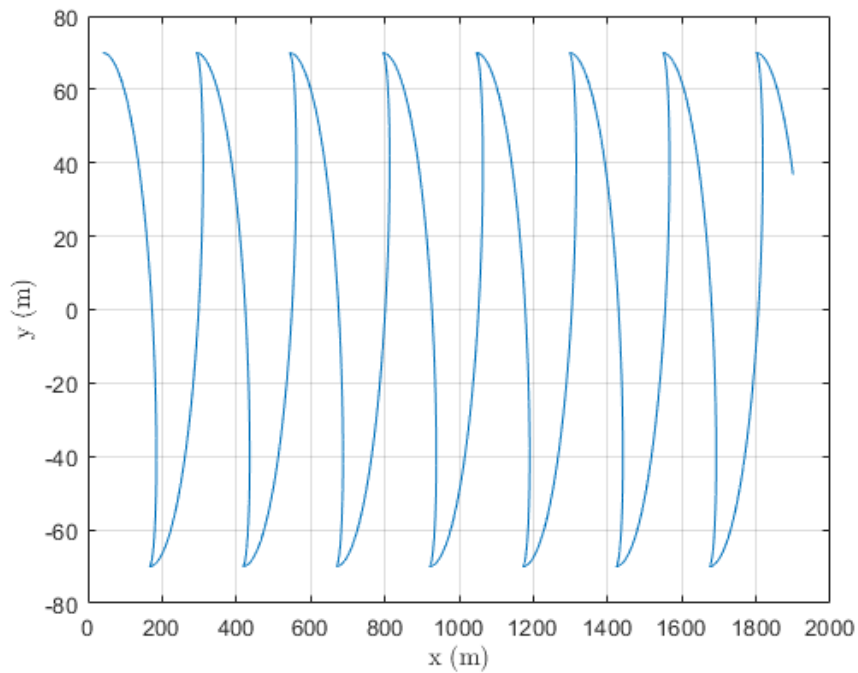

Figure 6.9: Coordinate z of the kite against time.

Figure 6.10: Coordinate x against coordinate y.

It can also be interesting to analyse the coordinates facing each other. If the coordinate x is represented versus the coordinate y, the shape of the circumference corresponding to the top view of the cylinder is observed. This circumference reaches an angle of rotation $\chi = 180°$, at which point, it changes its direction and repeats the course in the opposite way. As can be seen in figure 6.10, it does not have the shape of a semicircle corresponding to the movement described. This is due to the presence of the wind, which increases the coordinate x, leaving the coordinate y unchanged. The perfect semi-circumference would be described in a flight condition without wind.

In figure 6.11, the path of the kite is represented according to the coordinate x versus the coordinate z. The greater increase of x is observed as mentioned previously, likewise, certain peaks corresponding to the regressive part of the movement can be observed (when the kite moves backwards with respect to the wind). As the wind speed increases with respect to the tangential speed of the kite $\dot{\chi}R$, the peak will be smaller, because the regressive movement will be smaller.
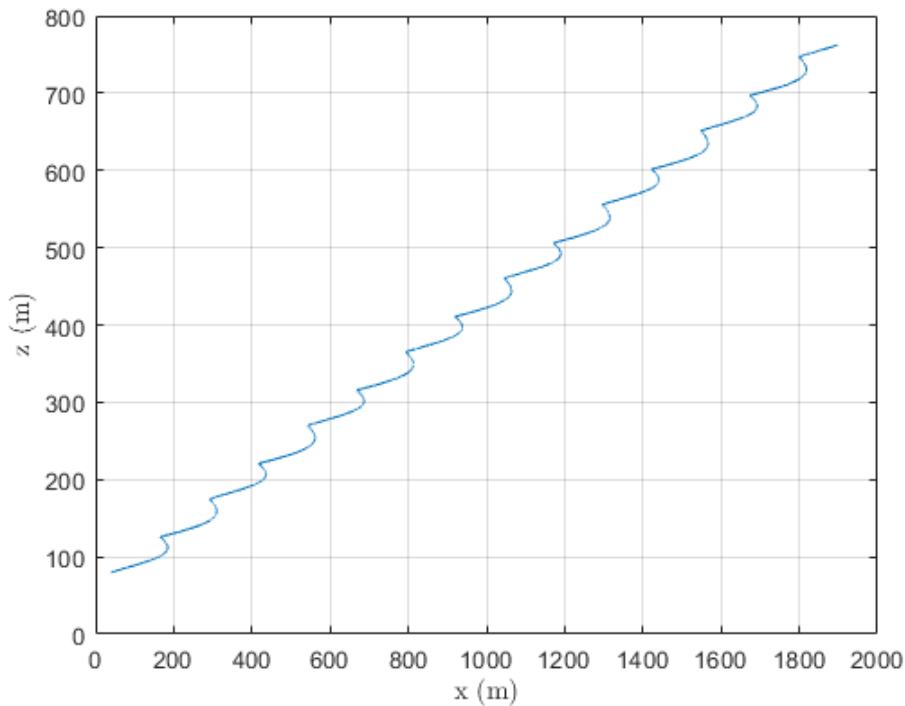

Figure 6.11: Coordinate x against coordinate z.

To finish the analysis of the opposite coordinates, the coordinate y is plotted against the coordinate z in figure 6.12. The sinusoidal evolution of the coordinate y is observed, while the coordinate z increases with it.
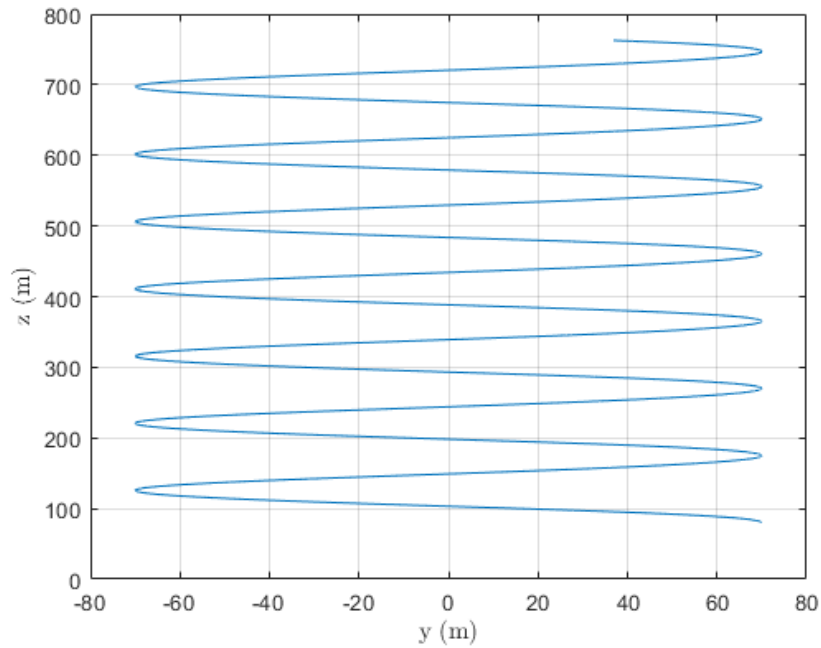
Figure 6.12: Coordinate y against coordinate z.

All these results of the trajectory are collected in figure 6.13, in which, the 3D trajectory is represented with the advance of time. It can be observed the clear change of direction each $\chi = 180°$, as well as the movement within a cylinder inclined an angle ε and radius constant R, because the coordinate y varies between $y_{max} = R$ and $y_{min} = -R$. Moreover, as previously mentioned, the movement is ascending and greater in the direction of the wind than in the other directions.

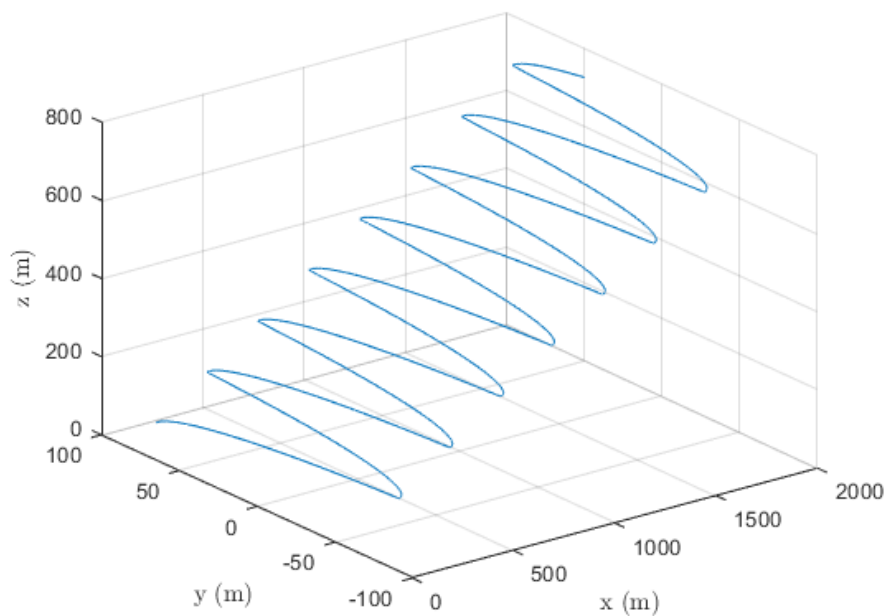Figure 6.13: Trajectory of the kite in 3 dimensions.

6.1.3. Angular positioning

The next step will be to position the kite with all the angles that contribute in the problem. The kite will be positioned with respect to the ground, as well as the body axes with respect to the wind axes, in which the equations of sum of forces and moments are solved. For this, the aerodynamic speed (indicated by the x_w axis) will be positioned with respect to the speed of the kite through the angle of sideslip β in the XY plane, and through the angle of attack α in the τb plane.

Afterwards, the inclined cylinder axis should be positioned with respect to the ground using the angle ε defined above (see equation 4.15). Besides, the aerodynamic velocity must be positioned with respect to the ground through the seat angle of the speed γ, as well as the speed of the kite with respect to the ground through the seat angle ϑ.

The last two angles analysed will be: the angle of rotation χ that positions the kite on the surface of the cylinder described when it makes the turn, and the roll angle μ that positions the lift of the kite with respect to its vertical.

6.1.3.1.   Angle of sideslip β

In figure 6.14, the evolution of the angle of sideslip along the trajectory of the kite is shown. A growth of said angle is seen with the increase of the angle of rotation χ until a point at which it begins to decay its value (the aerodynamic speed $\overrightarrow{V_{xy}}$ rotates less than the speed of the kite $\overrightarrow{V_{gxy}}$ in the XY plane). As expected, $\beta = 0°$ at the initial point because the aerodynamic speed and the speed of the kite are aligned and with the same sense.
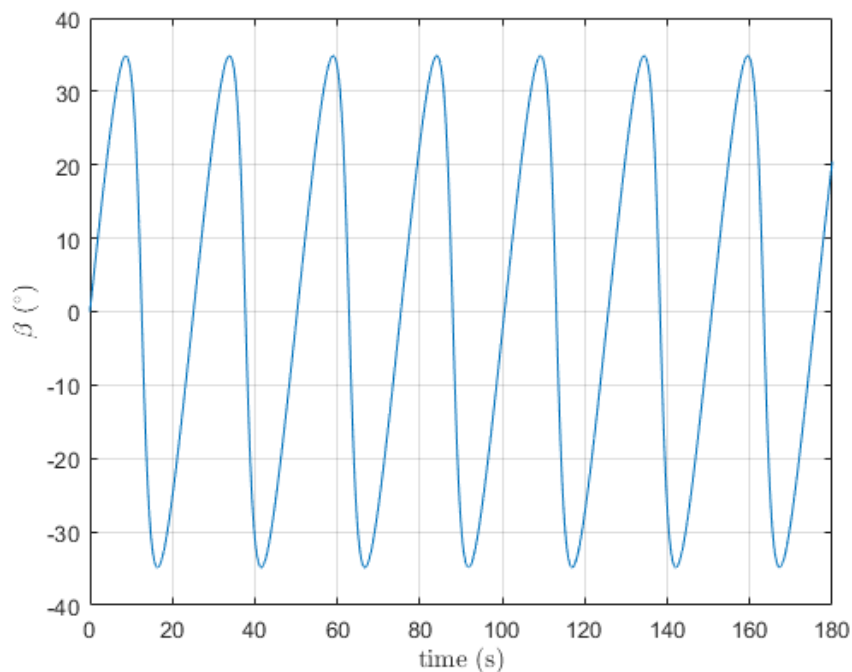

Figure 6.14: Angle of sideslip β against time.

However, when the angle of rotation $\chi = 180°$, the value of β depends on the intensity of both speeds.

$$\begin{cases} \beta = 0° & if \quad \dot{\chi}R > V_w \\ \beta = 180° & if \quad \dot{\chi}R < V_w \end{cases} \tag{6.6}$$

Furthermore, referring to the two intervals of equation 6.2, the angle of sideslip β is positive in the first intervals, and negative in the second one. This is due to the definition of the angle of sideslip β, which is defined as positive if the aerodynamic velocity is positioned to the right of the speed of the kite, and negative in the opposite case.

6.1.3.2.   Angle of the cylinder axis ε

In figure 6.15, the angle that forms the axis of the cylinder with respect to the ground is shown. This angle ε makes a great growth when the kite starts the movement to position the axis of the cylinder next to its equilibrium position. It is observed that the angle tends to a stationary value with slight oscillations with respect to that position due to the sinusoidal form of the movement.

This stationary value of the angle ε depends on the coordinate x and the coordinate z of the kite, and therefore, has a great dependence on the wind speed V_w as will be discussed later.
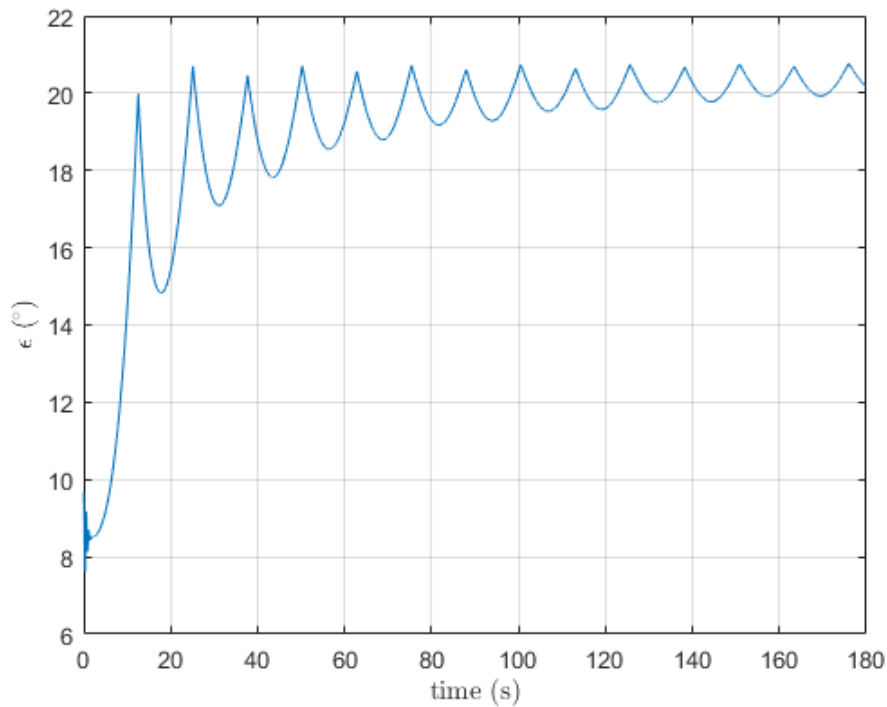

Figure 6.15: Angle of the cylinder axis ε against time.

6.1.3.3.   Seat angle ϑ

In figure 6.16, the evolution of the seat angle ϑ is shown, which represents the angle that forms the speed of the kite with respect to the ground. To simplify the problem and make a rotation around the cylinder almost constant, a constant seat angle ϑ has been chosen, whose value can be modified later if it is desired to make a faster or slower climb.

This angle will be key in the climb of the kite, since it includes the angle of attack α and the seat angle of the speed γ.
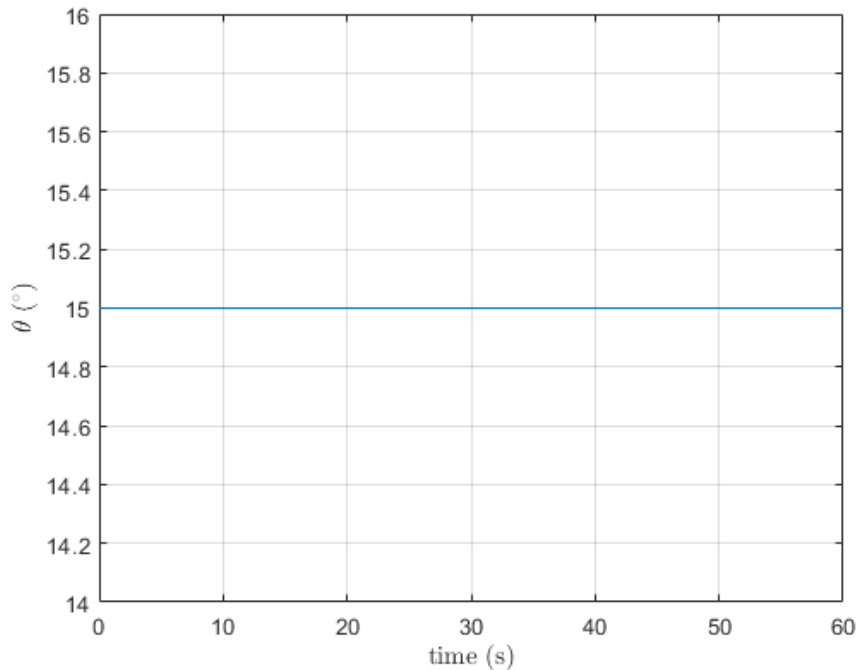

Figure 6.16: Seat angle ϑ (°) against time (s).

6.1.3.4.   Angle of attack α

In figure 6.17, the angle of attack α of the kite is represented, which measures the angle between the aerodynamic velocity and the speed of the kite in the τb plane. The angle of attack α has great importance in the calculation of the aerodynamic components, because the lift coefficient C_L depends on it (see equation 4.25), the coefficient of aerodynamic moment C_{mac} also depends on it through $C_{m\alpha}$ (see equation 4.27), and the aerodynamic drag coefficient C_D depends on the angle of attack α because it is a function of the lift coefficient (see equation 4.26) as well.

The angle of attack α starts with a null value as expected and trough a fast transient grows to a maximum value of $\alpha = 3.2°$. Once an angle of rotation $\chi = 180°$ has been reached, it begins to descend until it changes its direction again, and so on constantly. Care must be taken with this angle, because it cannot reach the angle of stall at any time since the lift would plummet and the equation 4.25 could not be applied anymore, and therefore, there will be a maximum attack angle α_{max} that will be slightly lower that the angle of stall α_{stall} as a precaution.
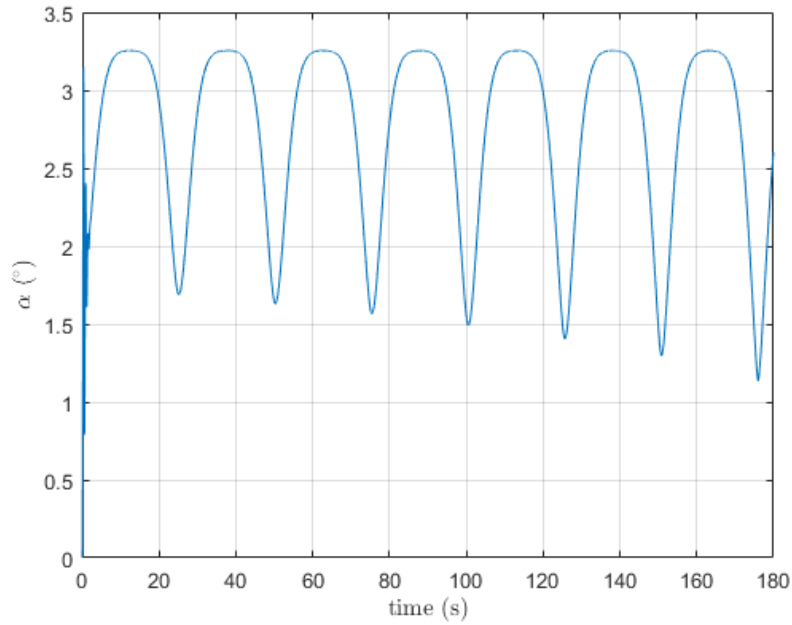
Figure 6.17: Angle of attack α against time.

After observing the variation of the angle of attack α, its angular speed $\dot{\alpha}$ should be positive when the angle of attack α grows, and negative when it descends as shown in figure 6.18. Moreover, this angular speed $\dot{\alpha}$ increases when the angular acceleration $\ddot{\alpha}$ of the attack angle α is positive, which occurs while the lift reduced with the $\cos\mu$ (roll angle) gives more positive moment than the aerodynamic moment M_a. Likewise, the angular speed $\dot{\alpha}$ decreases when the aerodynamic moment M_a provides more moment than the lift (negative angular acceleration $\ddot{\alpha}$). It also has an initial transient to achieve an almost null value.
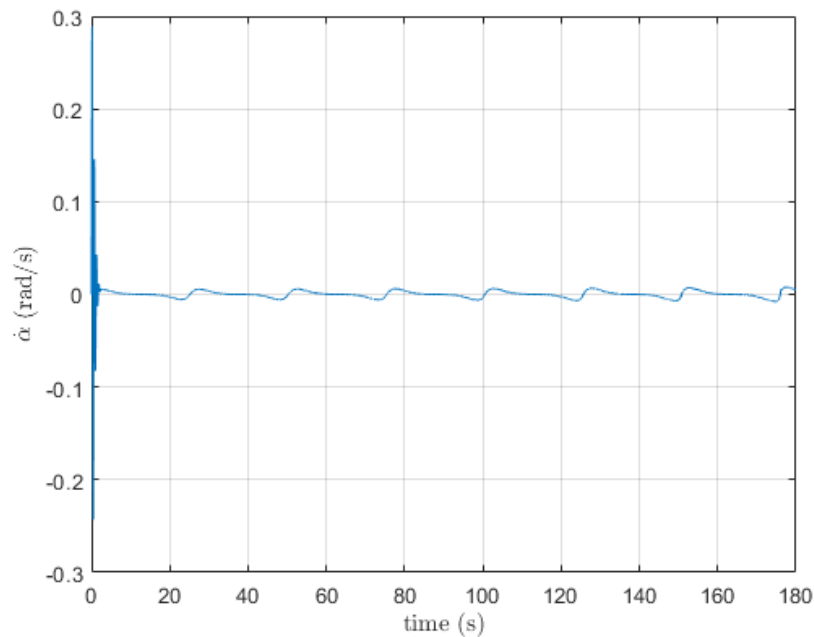

Figure 6.18: Angular speed of the angle of attack $\dot{\alpha}$ against time.

6.1.3.5.   Seat angle of speed γ

In figure 6.19, the seat angle of speed γ is represented, which measures the angle between the aerodynamic velocity and the ground. Fulfilling equation 4.23, the angle γ must start with a value $\gamma = 15°$ equal to the seat angle ($\vartheta = 15°$), because the initial attack angle α is zero. Afterwards, its trend must be opposite to the angle of attack α, decreasing until the angle of rotation $\chi = 180°$, then it starts to grow until reaching its initial value, and so constantly. It has a maximum value equal to the angle of seat, and a minimum value to satisfy the requirement of angle of attack α. It has the same initial transient as the angle of attack.

$$\begin{cases} \gamma_{max} = \vartheta - \alpha_{min} = 15° - 0° = 15° \\ \gamma_{min} = \vartheta - \alpha_{max} = 15° - 3.2° = 11.8° \end{cases} \tag{6.7}$$

The seat angle of the speed has great importance in the ascensional speed (see equation 4.5), and it will define together with the angle of sideslip β the trend of the trajectory because they position the aerodynamic speed.
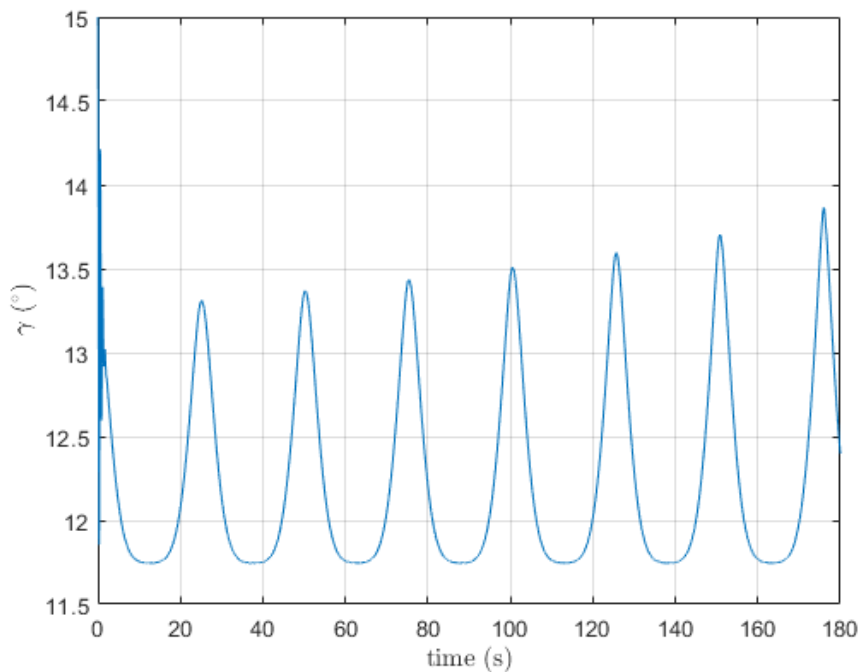

Figure 6.19: Seat angle of speed γ against time.

In figure 6.20, the angular speed of seat angle of the speed is shown. Its evolution is opposite to the angular speed of the angle of attack $\dot{\alpha}$. It begins descending with a negative value until its angular acceleration becomes positive, at which time it grows until it becomes null when the angle of rotation is $\chi = 180°$. After that, it continues growing until it reaches its maximum when the angular speed of the angle of attack $\dot{\alpha}$ is minimum and the angular acceleration of the first one becomes negative. It ends decreasing again until it nullifies its value and completes the cycle. It also has an initial transient to achieve an almost null value.
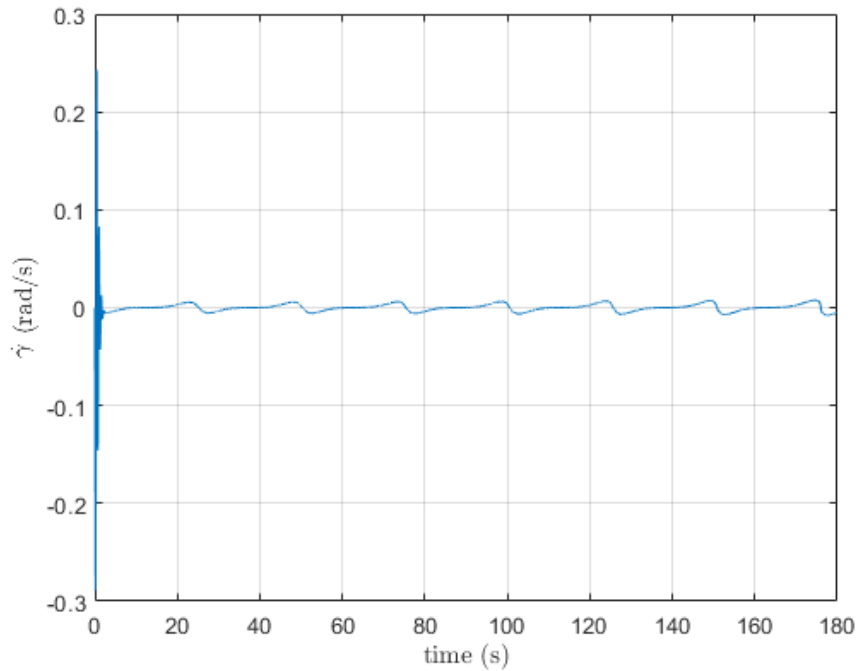
Figure 6.20: Angular speed of the seat angle of speed $\dot{\gamma}$ against time.

6.1.3.6.   Angle of rotation χ

Next, angle of rotation χ of the kite is shown in figure 6.21. It starts with null value and grows until it reaches its maximum value $\chi = 180°$, and then changes the sense of the kite and begins to decrease its angle of rotation χ until reaching the value $\chi = 0°$ again.

The growth of the angle is not linear, since it has an almost quadratic growth, because its angular speed $\dot{\chi}$ is not constant. Therefore, its growth will be lower at the beginning when its angular speed is lower, and it will grow faster when the angular speed $\dot{\chi}$ increases. This almost quadratic trend is due to the fact that its angular speed $\dot{\chi}$ is almost linear, as shown in figure 6.22. The angle of rotation χ will grow while its angular speed $\dot{\chi}$ is positive, which occurs in the first interval of movement (see equation 6.2), and will decrease when its angular speed $\dot{\chi}$ becomes negative (second interval).

The angular speed $\dot{\chi}$ has an almost linear trend, because its angular acceleration $\ddot{\chi}$ is almost constant. As discussed in chapter 6.1.1, the angular velocity $\dot{\chi}$ has an average value $\dot{\chi} = 0.25\ rad/s$, with a minimum value of $\dot{\chi} = 0\ rad/s$ and a maximum value of $\dot{\chi} = 0.5\ rad/s$. It becomes negative in the second interval of movement (see equation 6.2), in order to decrease the angle of rotation χ. The angular velocity $\dot{\chi}$ will grow when its angular acceleration $\ddot{\chi}$ (almost constant) is positive and will decrease when its angular acceleration $\ddot{\chi}$ is negative.
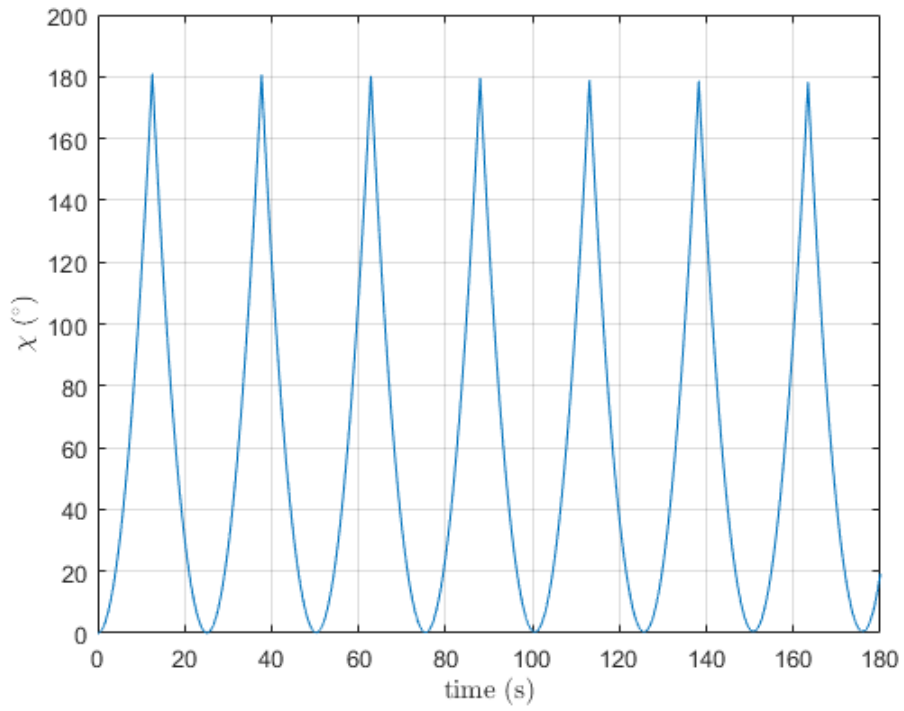
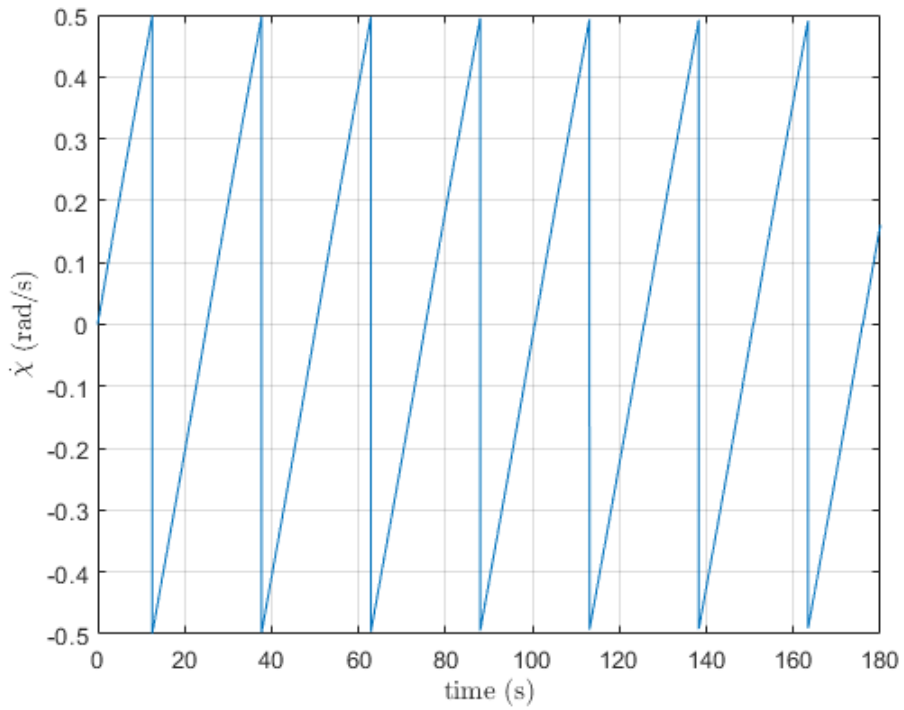Figure 6.21: Angle of rotation χ against time.

Figure 6.22: Angular speed of the angle of rotation $\dot{\chi}$ against time.

6.1.3.7.　　Roll angle μ

To finish with the angular positioning, the roll angle μ is shown in figure 6.23. This angle measures the inclination of the lift of the kite with respect to the vertical of the kite, or what is the same, the angle between the z_b body axis of the kite and the vertical of the kite. It is positive when it turns to the right of the z axis (vertical of the kite), and negative when it turns to the left of the z axis (vertical of the kite). Therefore, it will be positive in the first interval of the movement (see equation 6.2), and negative in the second one.

Its maximum value $\mu = 60°$ is obtained at the beginning of the movement with $\chi = 0°$, and then it is reduced until $\chi = 180°$, at which point it reaches its minimum value in the first interval. This minimum value depends on the speed of the wind and the tangential speed of the kite. There are three different conditions, but the first one does not have interest in this problem and cause some problems.

$$\begin{cases} \mu_{min} < 0° & with & V_w < \dot{\chi}R \\ \mu_{min} = 0° & with & V_w = \dot{\chi}R \\ \mu_{min} > 0° & with & V_w > \dot{\chi}R \end{cases} \qquad (6.8)$$

Afterwards, it continues to descend but with a negative value of the angle until it returns to the condition of $\chi = 0°$, at which point it completes the cycle. It also has an initial transient to achieve an almost null value.
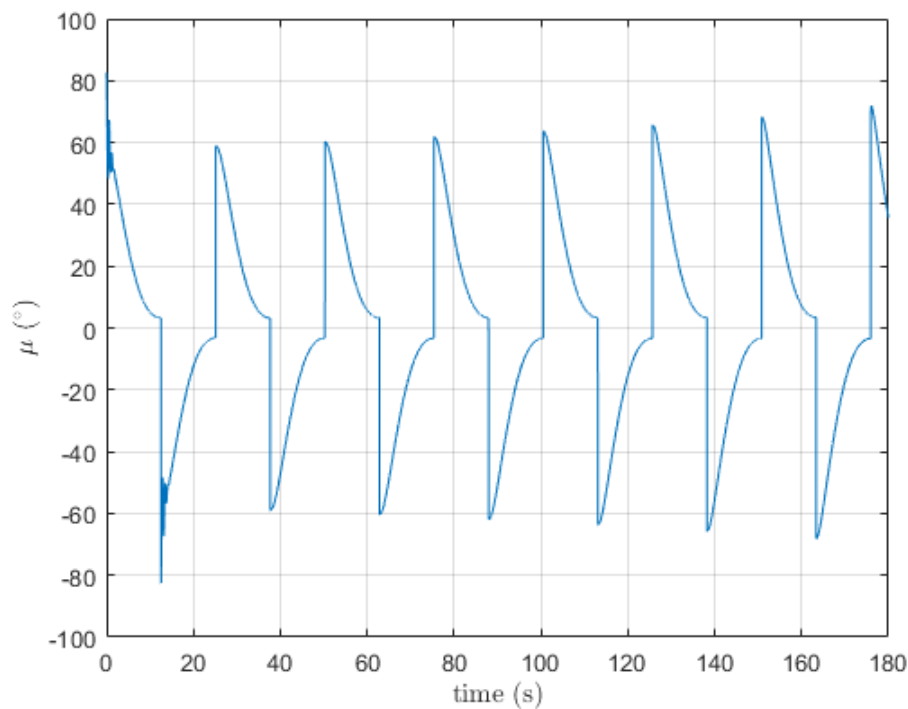

Figure 6.23: Roll angle μ against time.

61

6.1.4. Density results

Now, the variation of the air density ρ with the flight height h is shown in figure 6.24. As expected, as the flight height increases, the air temperature T decreases, and with this, the air density ρ decreases as well. In this case, the air density ρ changes from $\rho = 1.2147\ Kg/m^3$ at height $h = 80\ m$ to $\rho = 1.1385\ Kg/m^3$ at height of $h = 760\ m$. These values of air density ρ will be used in the calculation of the aerodynamic contributions.
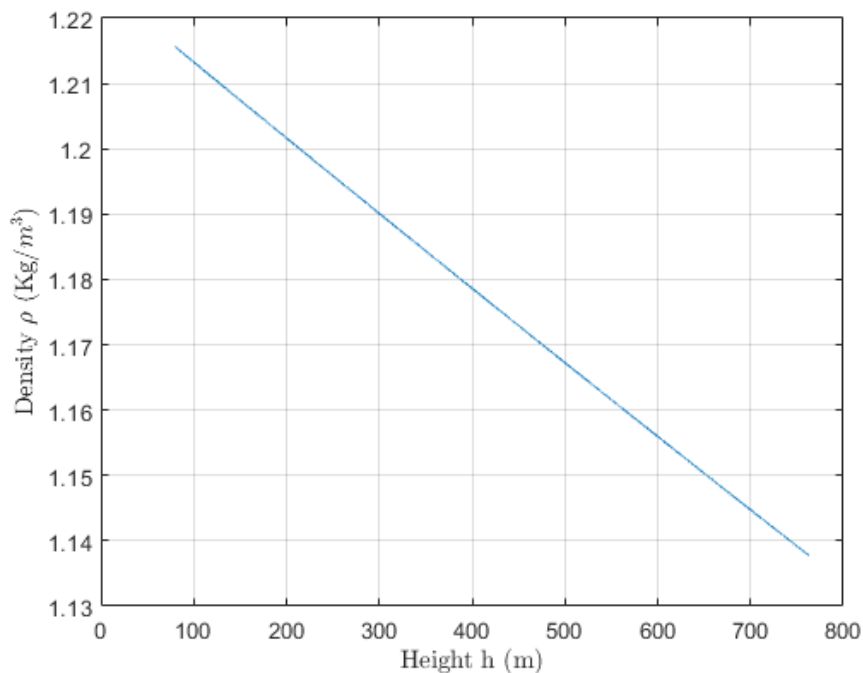

Figure 6.24: Density variation with height.

6.1.5. Aerodynamic results

To analyse the aerodynamic results, some parameters must be taken into account. First, the aerodynamic coefficients will be plotted, and then, using those coefficients, the aerodynamic forces and moment will be represented.

6.1.5.1.   Aerodynamic coefficients

The aerodynamic coefficients depend on the angle of attack and the deflection angle of the elevons. In this case, the deflection of the elevons will be assumed as zero and will be analysed in subsequent study about longitudinal stability. All the coefficients have an initial transient to achieve an almost periodic evolution.

In the figure 6.25 is represented the lift coefficient that varies as the angle of attack does. It has an initial value of $C_L = 0.7$ corresponding to the lift coefficient with angle of attack null C_{L0}. It has also a maximum value of $C_{Lmax} = 0.95$ approximately.

In the figure 6.26 is shown the aerodynamic drag coefficient that has a constant value corresponding to the drag coefficient without lift, and an induced drag that depends on the lift, and therefore, depends on the angle of attack. As it can be seen the drag is much lower than the lift, which entail an aerodynamic efficiency approximately $E = C_L/C_D = 18$.
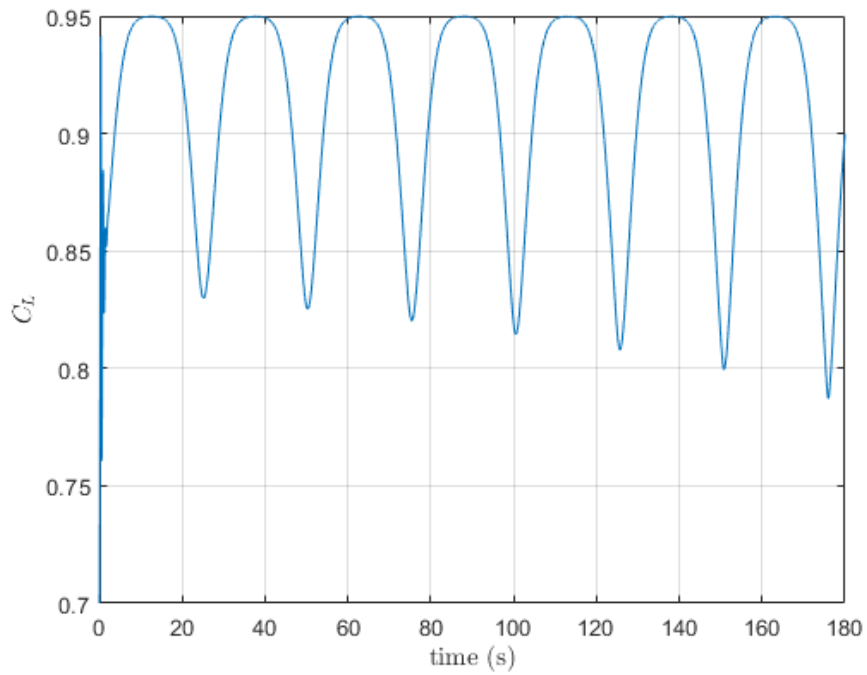
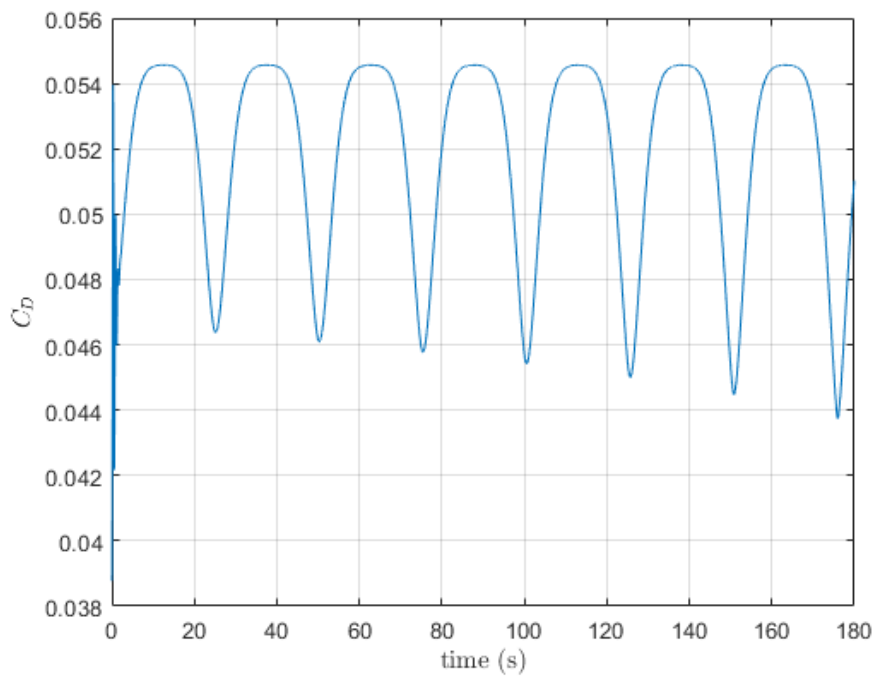Figure 6.25: Lift coefficient of the kite.

Figure 6.26: Aerodynamic drag coefficient of the kite.

The last coefficient analysed is the aerodynamic moment coefficient that is almost ever negative due to the $C_{m\alpha} < 0$ that allows a stable movement. When the $C_{m\alpha} > 0$, the kite is instable because the aerodynamic centre is behind the barycentre which makes impossible to control the kite. It has also an initial value corresponding to C_{m0}. The term that depends on the deflection of the elevons is null, because of the deflection is assumed as null.
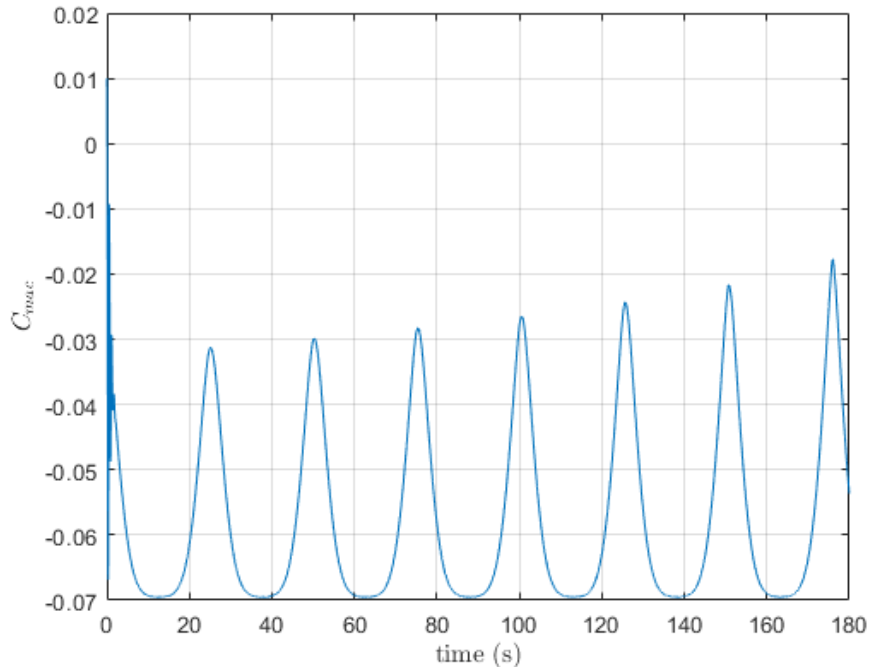

Figure 6.27: Aerodynamic moment coefficient of the kite.

6.1.5.2.   Aerodynamic forces and moments

Finally, the aerodynamic contributions are obtained from the aerodynamic coefficients, the wing surface, the aerodynamic speed and the density of the air. The lift, the aerodynamic drag and the aerodynamic moment have similar evolutions as their coefficients, but multiplicated with the parameters mentioned.

In the figure 6.28 is represented the lift, which has a minimum value when $\chi = 0°$ because in this point of the movement, the kite has a minimum angle of attack. It is also interesting to observe that vertical of the lift is very small when $\chi = 0°$, because the roll angle is very big. The opposite situation occurs when $\chi = 180°$, because the angle of attack is maximum, and the roll angle is minimum. The lift has an average value of 2600 N in this movement.

In the figure 6.29 is shown the aerodynamic drag that has a similar evolution to the lift due to the angle of attack influence, but in this case, the roll angle does not play any role in the drag. It has an average value of 150 N.

In both forces is observed a descent with the time, due to the decrease of the air density when the altitude grows. Besides, it can be seen an initial transient due to the angle of attack evolution.

In both forces, its value could be increased with a bigger wing surface, which entails a heavier kite too. Another option to increase the lift would be to increase the intensity (module) of the wind speed for obtaining an increase in the aerodynamic speed.
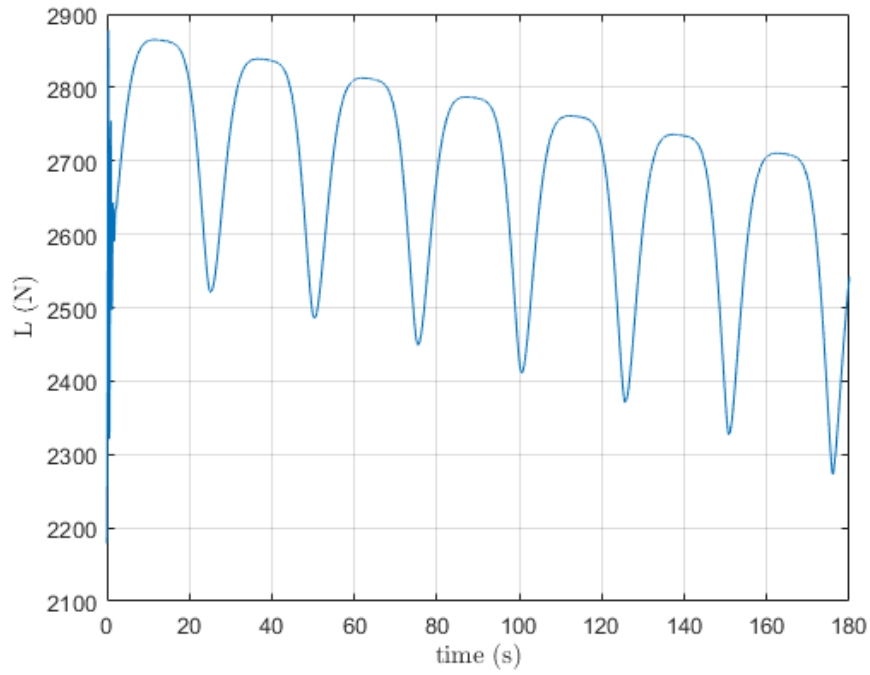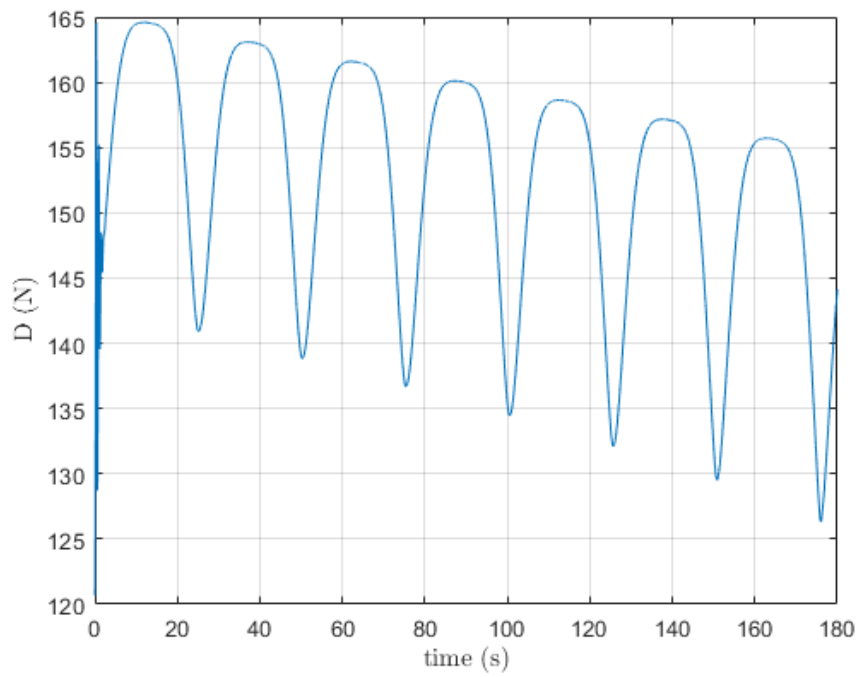
Figure 6.28: Lift of the kite.

Figure 6.29: Aerodynamic drag of the kite.

The last aerodynamic contribution is the aerodynamic moment that is shown in the figure 6.30. It must be negative to compensate the moment created by the lift carried out by the kite. Its evolution differs to the other two in the sign, and the influence of the mean aerodynamic chord in the aerodynamic moment that was not presented in the others.
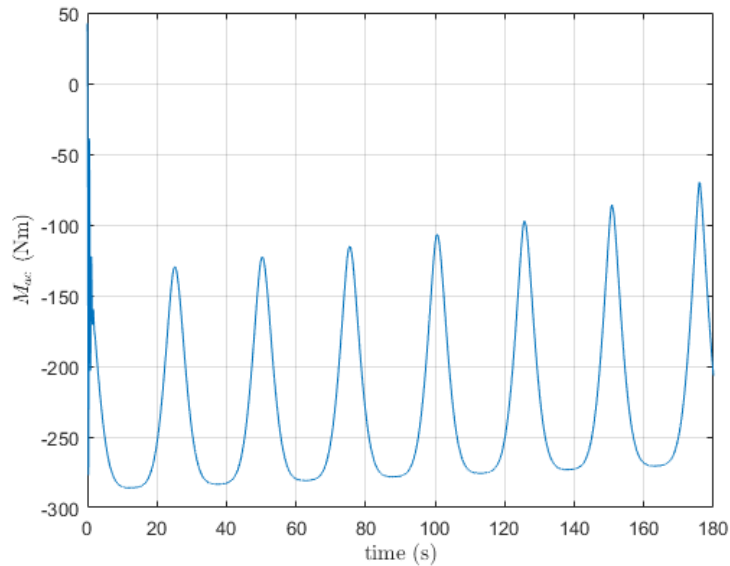

Figure 6.30: Aerodynamic moment of the kite.

6.1.6. Traction and Power calculation

To obtain the traction executed by the cable, is interesting to analyse the total length thereof, because its direction will indicate in which direction the total force must be projected. This length that is shown in the figure 6.31, depends on the three coordinates of the kite, and therefore, it has an important dependence of the wind speed because of the coordinate x.
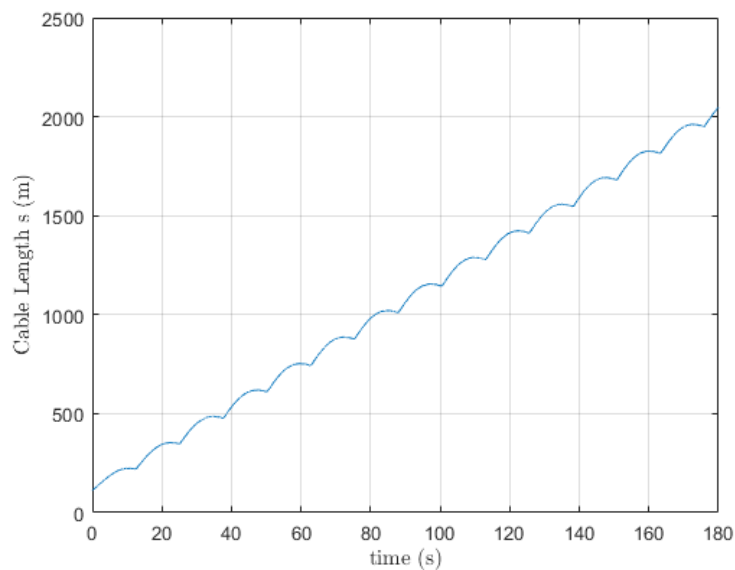

Figure 6.31: Cable length variation with time.

6.1.6.1.   Traction

In the figure 6.32 is plotted the traction executed by the kite which has a strange evolution. It is observed an incredible step at 12.566 s corresponding to the change of the direction of the kite. This step is due to the instantaneous change of direction which entails an instantaneous change in the roll angle too.

Some negative values are obtained due to the fact that the angle of attack incline the lift backwards in the opposite direction of the cable, moreover, the roll angle project the lift backwards. Besides, the aerodynamic drag and the weight oppose the lift.
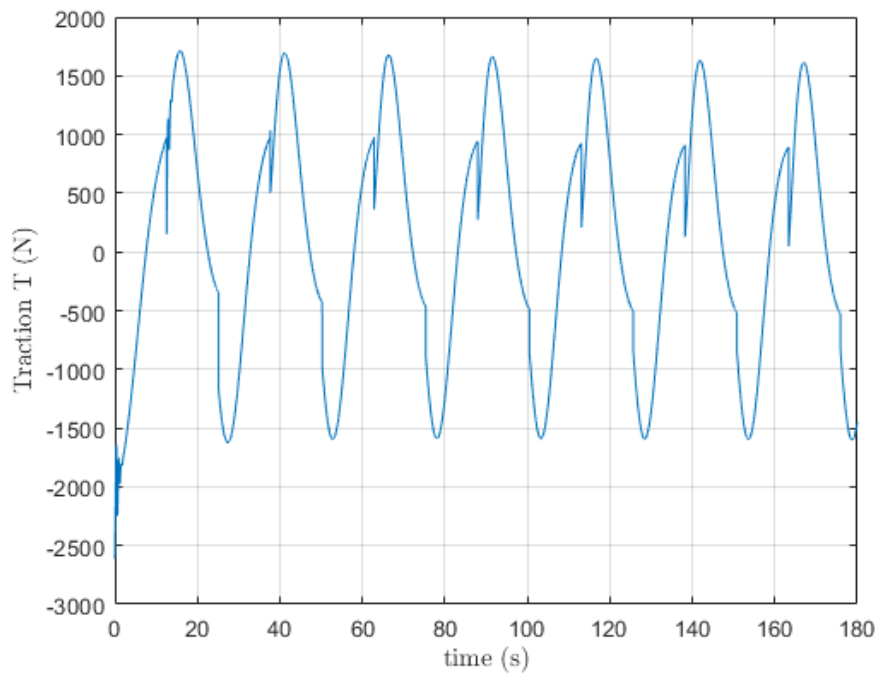

Figure 6.32: Traction executed by the cable.

6.1.6.2.   Power

Finally, the module of the traction is multiplicated for the unwinding speed to obtain the active power created by the kite in its ascending movement that is presented in the figure 6.33. It has an average value of $1614.8\ W$, and produces the following energy in the whole movement (180 s of simulation):

$$E_a = 0.0807\ kWh \qquad (6.9)$$

It is observed that the active power has some null values, because the traction has some negative values in which the unwinding speed is zero.

Then, the descent movement must be studied in a future to calculate the power consumed by the kite to return to its original position. The difference of both will be the available power created by the kite.
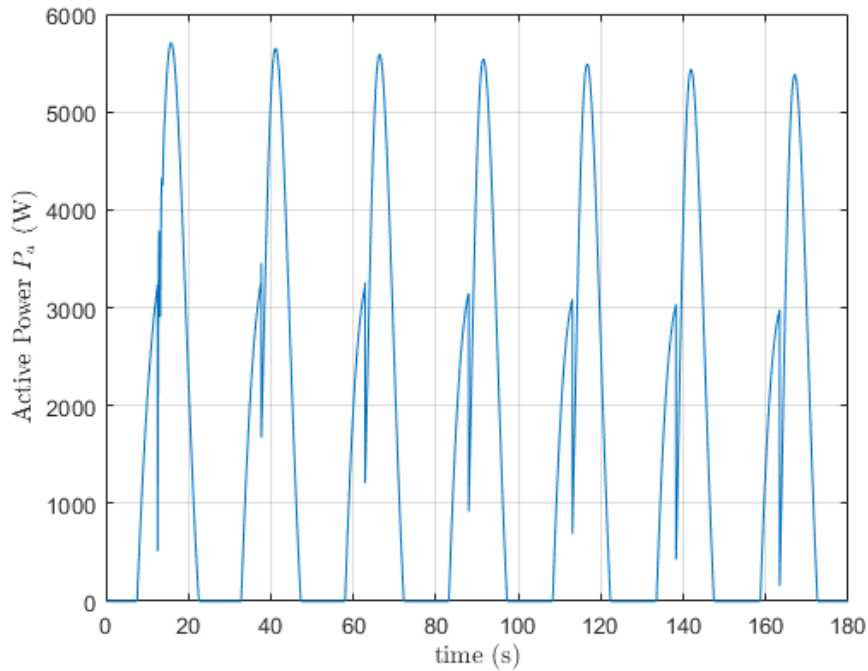
Figure 6.33: Active power created by the kite.

6.2. Variation of wind speed

To end the results chapter, it has been carried out a wind speed study. In the table 6.1 are presented the average active powers obtained for different values of wind speed. It is observed an almost linear increase of the active power when the wind speed grows. The order of magnitude of the average active power is around 1.615 kW for the expected wind. As expected, the kite does not produce power without wind.

Table 6.1: Power variation with wind speed.

V_w	P_a
$0\ m/s$	$0\ kW$
$1\ m/s$	$0.164\ kW$
$2\ m/s$	$0.330\ kW$
$3\ m/s$	$0.498\ kW$
$4\ m/s$	$0.662\ kW$
$5\ m/s$	$0.825\ kW$
$6\ m/s$	$0.988\ kW$
$7\ m/s$	$1.150\ kW$
$8\ m/s$	$1.312\ kW$
$9\ m/s$	$1.470\ kW$
$10\ m/s$	$1.615\ kW$

Chapter 7 - Conclusions

The first attempt was to suppose that the kite could carry out a trajectory in eight with constant altitude. This case was rejected because there was not an impulsive force to move the kite frontwards due to the wind was imposed as constant in module and direction. This movement could be feasible if an engine is joined to the kite to create a thrust. In any case, it does not have commercial sense, because the cable does not move, and therefore, it does not produce any power.

In the second attempt was supposed an ascending helix with constant turning radius and constant wind in the X direction. In this case, the kite produce power in some parts of its trajectory, when the traction executed by the kite is positive.

As expected, the kite could carry out the proposed movement in which it changes its direction when it reaches 180º in the angle of rotation. The trajectory and the positioning of kite have an enormous dependence of the wind speed because it is the impulsive force that generate the movement.

There are some restrictions in the model because the weight of the wing cannot be increased without a proportional increase on the wing surface. Another restriction could be the wind speed, that has the following mathematical limit (not physical limit):

$$V_w < \dot{\chi}_{average} R$$

Therefore, if the wind speed is increased, the product $\dot{\chi}_{average} R$ that is known as tangential speed must be increased too. The reason of these restrictions is that the model has several *asin(something)* and *acos(something)*, and the argument of this commands cannot be greater that 1 to have mathematical sense. Another restriction is a mass increase that must be followed of a turning radius increase, because a heavier kite cannot carry out the same trajectory due to the inertia created by its mass.

Finally, the wind study showed that the power created by the kite grows with the wind intensity as it was expected. There is a limit in the constant increase of the wind speed, because it cannot be increased as any want. The power could be also increased optimizing the ascending movement and the descending movement, or improving the efficiencies in the ground.

In a future study, some aspect should be analysed as the descent movement in which the kite consume power. Another point of interest could be the longitudinal stability, the directional stability and the lateral stability, with which the elevons and rudders are sized. A last kind of project might be a study of the trajectory of kite but describing a movement in eight in a crosswind condition.

Chapter 8 - Bibliography

[1] M. Á. Gómez Tierno, M. Pérez Cortés and C. Puentes Márquez, Mecánica del Vuelo. 2º Edition, Madrid: Ibergarceta Publicaciones, S.L., 2012.

[2] M. L. Loyd, "Crosswind Kite Power," *Journal of Energy,* vol. 4, no. 3, 1980.

[3] M. Granata and E. Mantia, "Avamprogetto di un velivolo ad ala fissa per lo sfruttamento dell' energia eolica in quota: analisi aeromeccanica e parametrica/ calcolo aerostrutturale," 2014.

[4] ISO International Standard 2533, Standard Atmosphere, Geneva, 1975.

[5] M. Diehl, "Airborne Wind Energy: Basic Concepts and Physical Foundations," *Springer,* pp. 3-22, 2013.

[6] R. Lozano Jr, M. Alamir, J. Dumon and A. Hably, "Control of a wind power system based on a tethered," *IFAC Workshop on Embedded Guidance, Navigation and Control in Aerospace,* vol. 45, no. 1, pp. 139-144, 2012.